



LUND UNIVERSITY

The Chirality-Flow Formalism and Optimising Scattering Amplitudes

Lifson, Andrew

2023

[Link to publication](#)

Citation for published version (APA):

Lifson, A. (2023). *The Chirality-Flow Formalism and Optimising Scattering Amplitudes*. [Doctoral Thesis (compilation), Department of Physics, Department of Astronomy and Theoretical Physics - Undergoing reorganization, Faculty of Science]. MediaTryck Lund.

Total number of authors:

1

General rights

Unless other specific re-use rights are stated the following general rights apply:

Copyright and moral rights for the publications made accessible in the public portal are retained by the authors and/or other copyright owners and it is a condition of accessing publications that users recognise and abide by the legal requirements associated with these rights.

- Users may download and print one copy of any publication from the public portal for the purpose of private study or research.
- You may not further distribute the material or use it for any profit-making activity or commercial gain
- You may freely distribute the URL identifying the publication in the public portal

Read more about Creative commons licenses: <https://creativecommons.org/licenses/>

Take down policy

If you believe that this document breaches copyright please contact us providing details, and we will remove access to the work immediately and investigate your claim.

LUND UNIVERSITY

PO Box 117
221 00 Lund
+46 46-222 00 00



The Chirality-Flow Formalism and Optimising Scattering Amplitudes

ANDREW LIFSON

FACULTY OF SCIENCE | LUND UNIVERSITY



The Chirality-Flow Formalism and Optimising Scattering Amplitudes

The Chirality-Flow Formalism and Optimising Scattering Amplitudes

by Andrew Lifson



LUND
UNIVERSITY

Thesis for the degree of Doctor of Philosophy

Thesis advisors: Malin Sjödal

Faculty opponent: Dieter Zeppenfeld

To be presented, with the permission of the Faculty of Science of Lund University,
for public criticism in Lundmarksalen at the Department of Physics
on Wednesday the 26th of April 2023 at 10:00.

Organization LUND UNIVERSITY Department of Physics Professorsgatan 1 SE-223 63 Lund Sweden		Document name DOCTORAL DISSERTATION	
Author(s) Andrew Lifson		Date of disputation 2023-04-26	
		Sponsoring organization	
Title and subtitle The Chirality-Flow Formalism and Optimising Scattering Amplitudes			
<p>Abstract</p> <p>This thesis is composed of five papers, which all attempt to optimise calculations of scattering amplitudes in high-energy-physics collisions. These scattering amplitudes are a key part of theoretical predictions for particle-physics experiments like the Large Hadron Collider at CERN. The first four papers are the main topic of the thesis, and describe a novel method called chirality flow. Chirality flow simplifies Feynman-diagram calculations and makes them more intuitive. Papers I, II, and IV describe chirality flow in detail at both tree-level and one-loop level, while paper III shows a first implementation of it in the event generator MadGraph5_aMC@NLO. The final paper instead explores the speed, accuracy, and precision of an approximation of the colour part of a scattering amplitude.</p> <p>Paper I introduces the chirality-flow formalism, a new pictorial method used to calculate tree-level helicity amplitudes by drawing lines and connecting them to find spinor inner products, instead of doing algebraic manipulations. This method makes calculations more transparent, and often allows one to go from Feynman diagram to spinor inner products in a single line. Massless QED and QCD are treated in full.</p> <p>Paper II extends the chirality-flow formalism of paper I to deal with massive particles, and therefore allows chirality flow to be used for any tree-level Standard Model calculation.</p> <p>Paper III describes our implementation of chirality flow in massless QED in MadGraph5_aMC@NLO. A speed comparison is made showing up to a factor of 10 increase in evaluation speed.</p> <p>Paper IV extends the chirality-flow formalism to the one-loop level for any Standard Model calculation, showing the simplifications in the numerator algebra and the tensor reduction.</p> <p>Paper V describes an extension to the MadGraph5_aMC@NLO event generator in which the kinematics are calculated using Berends-Giele recursions instead of Feynman diagrams, and the colour matrix can be expanded in the number of colours N_c. The speed of the extension, and the accuracy and precision of the colour expansion are explored.</p>			
Key words Spinor-Helicity Formalism, Chirality-Flow Formalism, Helicity Amplitudes, Standard Model, QED, QCD, Optimisations, Colour Expansion, Phenomenology			
Classification system and/or index terms (if any)			
Supplementary bibliographical information		Language English	
ISSN and key title		ISBN 978-91-8039-588-5 (print) 978-91-8039-589-2 (pdf)	
Recipient's notes	Number of pages 268	Price	
	Security classification		

I, the undersigned, being the copyright owner of the abstract of the above-mentioned dissertation, hereby grant to all reference sources the permission to publish and disseminate the abstract of the above-mentioned dissertation.

Signature _____

Date 2023-02-14

The Chirality-Flow Formalism and Optimising Scattering Amplitudes

by Andrew Lifson



LUND
UNIVERSITY

A doctoral thesis at a university in Sweden takes either the form of a single, cohesive research study (monograph) or a summary of research papers (compilation thesis), which the doctoral student has written alone or together with one or several other author(s).

In the latter case the thesis consists of two parts. An introductory text puts the research work into context and summarises the main points of the papers. Then, the research publications themselves are reproduced, together with a description of the individual contributions of the authors. The research papers may either have been already published or are manuscripts at various stages (in press, submitted, or in draft).

Cover illustration front: Lund University Library, October 2022.

Cover illustration back: Picture of me in front of my whiteboard, March 2023.

Funding information:

This work was supported by the Swedish Research Council (contract no. 2016-05996), as well as the European Union's Horizon 2020 research and innovation programme (grant agreement no. 668679). This work has also received funding from the European Union's Horizon 2020 research and innovation programme as part of the Marie Skłodowska-Curie Innovative Training Network MCnetITN3 (grant agreement no. 722104).

© Andrew Lifson 2023

Faculty of Science, Department of Physics

ISBN: 978-91-8039-588-5 (print)

ISBN: 978-91-8039-589-2 (pdf)

Printed in Sweden by Media-Tryck, Lund University, Lund 2023



“It is trivial, but profound.”

Dr. David M. Paganin

Contents

Acknowledgements	v
List of publications	vii
Popular Summary	viii
Introduction	I
1 A General Overview: Particle Physics, the Standard Model, and the Role of this Thesis within it	3
2 The fundamentals of Particle Physics	9
2.1 The Lorentz Group, Mass, and Spin	9
2.1.1 Wigner's little group	11
2.2 Lagrangians	14
2.3 Particle Wavefunctions	15
2.4 Gauge Fixing	18
3 Scattering Amplitudes and How to Calculate Them	18
3.1 Textbook method to Calculate a Scattering Amplitude	20
3.2 The Spinor-Helicity Formalism	22
3.2.1 Massless Particles	22
3.2.2 Massive Particles	26
3.3 Berends-Giele Recursions	27
4 QCD and Colour	29
4.1 Expansion in the Number of Colours	30
4.2 Colour Flow	31
5 Automating Scattering Amplitudes using MadGraph5_aMC@NLO	32
5.1 HELAS	33
5.2 UFO Models and Diagram Generation	36
5.3 ALOHA	37
6 Loop Calculations	38
6.1 Divergences	38
6.2 Dimensional Regularisation	40
6.3 The FDF Formalism	42
6.4 Tensor Reduction and Master Integrals	43
7 Conclusions and Outlook	44

8	Overview of Publications in this Thesis	47
9	Overview of Work not in this Thesis	49

Publications

I	The chirality-flow formalism	63
1	Introduction	64
2	Color flow	66
3	The basics of the spinor-helicity formalism	67
3.1	Spinors and spinor inner products	67
3.2	Four-vectors	70
3.3	Polarization vectors	72
4	Building the chirality-flow picture	73
4.1	A simple QED example	73
4.2	Proof for QED	76
4.3	Proof for QCD	77
4.4	QCD remarks	78
5	Chirality-flow Feynman rules	79
5.1	Vertices	79
5.2	Propagators	84
5.3	Application	85
6	Examples	87
6.1	$e^+e^- \rightarrow \mu^+\mu^-$	87
6.2	$e^+e^- \rightarrow \mu^+\mu^-\gamma$	88
6.3	$q_1\bar{q}_1 \rightarrow q_2\bar{q}_2g$	90
6.4	$q\bar{q} \rightarrow g\bar{g}$	95
6.5	$g\bar{g} \rightarrow g\bar{g}$	98
7	Conclusion and outlook	100
A	Conventions and identities	102
A.1	Pauli matrices	102
A.2	Spinors and spinor inner products	103
A.3	Four-vectors and bispinors	105
A.4	Tables with QED and QCD conventions and Feynman rules	108
II	The chirality-flow formalism for the standard model	119
1	Introduction	120
2	Massless chirality-flow	120
2.1	Weyl spinors	121
2.2	Massless fourvectors	122
2.3	Polarization vectors	124
2.4	Linking objects	125
3	The chirality-flow formalism with massive particles	125

3.1	Spin and helicity	125
3.2	Massive fourvectors	126
3.2.1	Helicity and the eigenvalue decomposition	127
3.3	Dirac spinors from massless Weyl spinors	128
3.3.1	Helicity eigenstates	130
3.4	Polarization vectors	130
3.4.1	Helicity eigenstates	132
4	Chirality-flow Feynman rules with massive particles	132
4.1	Vertices	133
4.1.1	Triple vertices	133
4.1.2	Four-boson vertices	135
4.2	Propagators	136
4.3	Chirality-flow arrows and signs	137
4.4	Application	139
5	Examples	140
5.1	$e^+e^- \rightarrow \gamma\gamma$	140
5.2	$e^+e^- \rightarrow Zh$	141
5.3	$q\bar{q} \rightarrow q\bar{q}h$	143
6	Conclusion and outlook	145
A	Dirac spinors	146
A.1	Conventions and the chiral representation	146
A.2	Relativistic spin operator for massive spinors	147
B	Weyl spinors	149
B.1	Explicit representations of spinors and their inner products	149
B.2	Useful Identities	150
C	Tables with conventions and Feynman rules	151
III	Automating scattering amplitudes with chirality flow	163
1	Introduction	164
2	Chirality flow	165
3	MadGraph implementation	168
4	Results	169
5	Conclusion and outlook	170
IV	One-loop calculations in the chirality-flow formalism	179
1	Introduction	180
2	Introduction to chirality flow	181
3	FDF	185
4	Flowing loops	187
4.1	Reduction of tensor integrals	192
4.2	Abelian gauge theories	193
4.3	Non-abelian gauge theories	200

4.3.1	QCD	200
4.3.2	Other non-abelian theories	202
5	Conclusion	203
A	Additional chirality-flow rules	204
V	Improving Colour Computations in MadGraph5_aMC@NLO and Exploring a	
	1/N_c Expansion	215
1	Introduction	216
2	Background Theory	217
2.1	Colour Ordering and the 1/ N_c Expansion	217
2.1.1	Colour Ordering in the Fundamental Basis	217
2.1.2	1/ N_c Expansion	219
2.2	Berends-Giele Recursions	221
3	Technical Implementation	223
3.1	The MadGraph5_aMC@NLO Event Generator	223
3.2	Implementation of Colour Computation	223
3.3	Implementation of Berends-Giele Recursion	225
3.4	Sources of Speed Differences	227
4	Validation and Results	228
4.1	Accuracy and Precision of Colour Approximation	229
4.2	Speed Gain	233
5	Conclusion	238
A	Manual	239
B	Accuracy and Speed of Additional Processes	240
C	Subprocess Cross-Sections in Multi-Jet Production	243
D	Modified Colour Expansion for Multiquark Amplitudes	244

Acknowledgements

There are many people I would like to thank and acknowledge for helping me get to and write this thesis. First and foremost, I would like to thank both of my parents, especially Mum, for all of the help and encouragement to make sure that I worked hard and managed to achieve my dreams of travel, seeing World Cups, studying physics for a living, and living abroad. I could not think of a better possible upbringing and family, and am sorry that most of my dreams meant being on the other side of the world to you.

I would also like to express my large and sincere gratitude to my supervisor, Malin Sjödhall, for the opportunity to work on a fun project, the encouragement to pursue the opportunity to work on MadGraph in Belgium, your patience while I worked in the student unions, and for many stimulating physics discussions. Your idea which became chirality flow and this thesis was inspired, and I wish you the best of luck for both your and its future. I would also like to thank my other collaborators on this project, Adam, Christian, Emil, Joakim, Simon, and Zenny, for their talented inputs, hard work and enthusiasm. Additionally, I would like to thank both the European and Swedish research councils (ERC and VR respectively) for funding my research.

I would like to thank Olivier Mattelaer for a very nice collaboration, for helping teach me useful computer tricks, for giving me a start in MadGraph, and for always being encouraging and kind. Additionally, I would like to thank Fabio, Rikkert, Stefano, and Timea for their help and interesting discussions during this project.

For giving me my first opportunity in particle physics and event generators as an honours student, for being patient with a then computer-illiterate student, for being a selfless mentor, and for always welcoming me back to Monash, I would like to strongly thank Peter Skands. I do and will always greatly appreciate everything you have done for me.

To everyone at theoretical particle physics at Lund, I would like to thank you for the nice, social atmosphere I have experienced here, especially in my first year when I was still settling in. Of the seniors, I would like to thank Hans, Gösta, Johan, Leif, and Stefan for various bits of help and advice, and Torbjörn for first telling me about the PhD position. I would like to thank all of the postdocs, as each of you helped make life more fun here. Additionally, I would like to all of my fellow PhD students for the fun, encouragement, help, and for not experiencing this alone. While I am thanking all of you, I would like to especially thank Marius for being an awesome office mate, engaging in fun and stimulating discussions, and helping me settle in; Timea for being a fun office mate, for the helpful discussions on MadGraph and colour, and for nice companionship during and on the way to conferences and schools we both went to; Robin for the many fun social events, discussions, and the occasional Simpsons quote; Chiara for becoming my local football friend, and giving me many of my favourite Brazilian foods; Mattias for all of the interesting help and discussions

on local culture, language, and systems; and Leif, Smita, Astrid, and Nils for being so welcoming and helping me settle in when I first arrived. Finally for our division, I would like to thank Rikkert and Mattias for taking the time to read the first draft of this thesis and providing helpful feedback.

For the many fun trips on which I learned valuable soft skills and physics, and met many interesting people, as well as for funding my stay at UC Louvain, I would like to thank MCnet. I would also like to thank my fellow MCnet student and postdoc committee members for their good and hard work, especially Smita, Conor, and Pratixan, the latter two for helping me set up the MCnet youngsters journal and computer club, which I hope will continue to be interesting and useful.

I would like to thank Smita for encouraging me to join the world of student representation at Lund University. Thanks to her I gained fun and valuable experience at both NDR and LDK, learning about the university and my own leadership capabilities, and working with excellent people like Smita herself, Brian, Bibi, Leif, Linnea, Lea, and Vincent. Thanks to all of you for helping me as chair and vice chair, and in various other capacities.

To my Australian friends and family, I want to thank you for putting up with me always being abroad and for staying in contact. I look forward to once gain being a part of your physical lives.

To my housemates during the first three years, thank you for your kindness and flexibility, and for making my life outside of my PhD more fun. I especially want to thank Cyrille for being so fun, David for being flexible with rent when I lived in Copenhagen during the pandemic, and Matylda and Oliwia for allowing me to stay with them and Ewa in Copenhagen during the pandemic.

Last, but absolutely not least, I would like to thank Ewa, who has been with me for most of the PhD. She kept me sane during the pandemic, helped me relax when otherwise working too hard, looked after me during stressful moments, helped me clarify my life goals, taught me so many useful life skills and interesting cultural facts, introduced me to her family in rural Poland who immediately made me feel at home despite us not speaking the same language, and was a brilliant help during a difficult period. Ewa, I love you so much, and can't wait to start our next chapters together; first our travels through Central and North America, and the Caribbean, and then beginning our life together in the real world in Melbourne.

List of publications

This thesis is based on the following publications, referred to by their Roman numerals:

- I **The chirality-flow formalism**
Andrew Lifson, Christian Reuschle, and Malin Sjö Dahl
Eur.Phys.J.C 80 (2020) 1006. E-print: arXiv:2003.05877 [hep-ph]

- II **The chirality-flow formalism for the standard model**
Joakim Alnefjord, Andrew Lifson, Christian Reuschle, and Malin Sjö Dahl
Eur.Phys.J.C 81 (2021) 371. E-print: arXiv:2011.10075 [hep-ph]

- III **Automating scattering amplitudes with chirality flow**
Andrew Lifson, Christian Reuschle, Malin Sjö Dahl, and Zenny Wettersten
Eur.Phys.J.C 82 (2022) 535. E-print: arXiv:2203.13618 [hep-ph]

- IV **One-loop calculations in the chirality-flow formalism**
Andrew Lifson, Simon Plätzer, and Malin Sjö Dahl
To be submitted to Eur.Phys.J.C. E-print: arXiv:2303.02125 [hep-ph]

- V **Improving colour computations in MadGraph5_aMC@NLO and exploring a $1/N_c$ expansion**
Andrew Lifson and Olivier Mattelaer
Eur.Phys.J.C 82 (2022) 1144. E-print: arXiv:2210.07267 [hep-ph]

Popular Summary

This thesis is the culmination of my four and a half years of research in theoretical particle physics at Lund University (with a short stay at UC Louvain, in Belgium, included). For the majority of this thesis I describe a new method called chirality flow, which I developed along with my supervisor and collaborators to calculate the scattering probabilities of colliding fundamental particles at high energies more efficiently and transparently. Additionally, I optimised a part of the computer program `MadGraph5_aMC@NLO` which calculates these scattering probabilities. But what does this mean? Why did I do this? And how successful were these methods?

To answer the first two questions, we must first understand the basics of particle physics. The aim of theoretical particle physics is to find and study the smallest, most fundamental building blocks which make up our universe. That is, if you were to take an object around you and break it into ever smaller and smaller pieces, would you eventually find some fundamental particle which cannot be further broken up? If so, what would these particles look like, and how would they behave? To the best of our knowledge so far, it appears as if everything can be created by a set of 17 distinct particles which interact with each other via gravity, and at least one of the other three fundamental forces of nature: electrodynamics (QED), responsible for electricity and magnetism; the weak force, which is partially responsible for radioactivity and radioactive decay; and the strong force, also called quantum chromodynamics (QCD), which binds together protons and neutrons in the atom. Together, these 17 particles, their properties, and their interactions, make up the Standard Model of particle physics.

In the opening paragraph, I said that I calculated scattering probabilities, that is, the probability of two fundamental particles colliding and creating some final set of particles with a given set of momenta. Notice that I said scattering *probabilities*, not *the* outcome of a given scattering event. This is because fundamental particles are extremely small and obey the laws of quantum mechanics. Therefore, they are probabilistic rather than deterministic. That is, given a single starting point, there are multiple possible things which may happen, each with a certain probability to occur, rather than one single possible outcome.

To understand what these particles look like and how they behave, we have to first break up some object to both create them and to make them interact with each other. The best tool we have to do so today is the Large Hadron Collider (LHC) at CERN, which smashes together protons at extremely high energy and measures what is created. Since what is created follows a probabilistic distribution, we need to smash together very many protons to obtain enough statistics to determine the probability of a certain outcome. Next, we compare this distribution to the distribution calculated according to the rules of the Standard Model. If the experimental and theoretical distributions match, we say that the result confirms the

Standard Model, and if there is a discrepancy, we must find a new explanation, possibly involving new types of particles.

In order to calculate the theoretical prediction, we calculate the scattering probability of two protons becoming some final state with some momenta, and repeat this process possibly millions of times with different random final-state particles and momenta. For complicated final states, this requires a great deal of (expensive) computer power, and optimising it is very desirable. In this thesis, we attempted to optimise this task in several ways, including developing the chirality-flow formalism.

The third question, was how successful were the methods? Using chirality flow with pen and paper, we were able to do known calculations in less time than using previous methods, and it became much easier to see what part of the calculation led to what part of the result. When implementing chirality flow in the computer program `MadGraph5_aMC@NLO`, we found significant speed-ups in simulation time, thus proving chirality flow to be a success. Additionally, I optimised an unrelated component of `MadGraph5_aMC@NLO` called the colour sum, successfully making it two times faster than before. This is important, because the colour sum often uses the most computer resources in a given calculation.

There are five papers in this thesis. In the first two papers, I, along with my supervisor and collaborators, developed a formalism called chirality flow which requires less work and is more transparent than standard calculation methods. We developed this for the most basic approximation possible, known as tree-level. We did the calculations with pen and paper rather than on a computer, marvelling in the beauty, simplicity, and transparency of chirality flow compared to standard methods. Then, in paper III, we implemented this method in the computer program `MadGraph5_aMC@NLO`, making its QED calculations up to 10 times faster than before. In paper IV we extended the previous papers, developing chirality flow for the next-to-most-basic approximation, called one-loop level. Finally, in paper V, I sped up the leading bottleneck of `MadGraph5_aMC@NLO` by about a factor of 2, and while doing so learned enough about the program to complete paper III.

In addition to the work included in this thesis, over the four and a half years of my PhD I worked on several things not included in this thesis, including talks, seminars, proceedings, co-supervising a bachelor student, work for the student unions, and representing students and postdocs in the Monte Carlo network (MCnet) board, a funding agency and international collaboration working on simulations in particle physics. I also have ongoing work, in which I, along with the other authors of paper III and some master students, are working to implement chirality flow for the rest of the Standard Model in `MadGraph5_aMC@NLO`. While not directly a part of this thesis, these works were still an important part of my time in this PhD.

Introduction

This thesis is the culmination of over a decade of hard work, and is the crowning achievement of my work-life so far. Since first learning in high school about the wonderful weirdness of special relativity and quantum mechanics, I have wanted to study physics or mathematics for a living. To do this, I have worked very hard, first at Monash University to get both the understanding and the grades required to pursue this dream, and then at ETH Zürich and École Polytechnique to gather the necessary technical background required to do high-level research at a good pace. Finally, for the last four and a half years at Lund University and UC Louvain, I have fulfilled my dream of working as a scientist and getting a PhD in particle physics.

In my mid twenties, after having travelled to many parts of the world, I also had a dream of living overseas and trying out a different lifestyle and culture. I am extremely grateful that through physics, I was able to live in Zürich, Paris, Lund, Copenhagen, Louvain-la-Neuve, and Malmö, a set of experiences which have helped shape me as a person and enabled me to meet many great people, see many wonderful sights, and experience many new cultures. For this, I also want to thank both the universal nature of physics (assuming one can thank such an inanimate and intangible thing), and those who accepted me into the Master and PhD programs, allowing me to complete two dreams at one time.

Therefore, this thesis is extremely special to me. While I am aware that the most likely job of this thesis after I have defended it will be to sit on bookshelves collecting dust, I hope that it is nevertheless a useful and valuable document to many people. To my friends and family, I hope that this thesis starts off at such a level that you can roughly understand what I have been doing for a living so far. To my colleagues, past, present, and future, I hope that this thesis is a useful collection of background theories and cutting-edge research which can be used as the basis to understand scattering amplitudes, the spinor-helicity formalism, chirality flow, MadGraph5_aMC@NLO, colour expansions, and some one-loop techniques. Finally, to me, I would love for this thesis to take on the function of a photo album, a collection of memories and experiences in a single tome, that I can pick up from time to time and remind myself of all of the experiences, positive and negative, that were had in

my four and a half years as a PhD student.

This thesis is structured as follows: We begin in section 1 with an overview of what particle physics is, and the role my thesis plays in this vast research field. This first section aims to be understandable to everyone, no matter their background. We start off with the basics, understanding length and energy scales, and what we mean by a particle and its properties. From this, we describe the Standard Model of particle physics, its forces and how we test them. Finally, we put this thesis into context.

From section 2 onward, we assume some background knowledge of physics. We begin this section by describing the fundamentals of particle physics, reminding about the Lorentz group and how it is responsible for a particle's mass and spin. In particular, we describe the subgroup of the Lorentz group called the little group, which is responsible for spin. We briefly remind some of the main ideas of Lagrangians, describe particle wavefunctions and their properties, and then finish the section with a short discussion on gauge fixing in propagators.

In section 3, we give an overview of scattering amplitudes, placing the work of this thesis into sharper context. We begin by reminding about the perturbative expansion and how we calculate within it. We describe how scattering amplitudes are typically calculated in textbooks, why the textbook method is inefficient, how to use the spinor-helicity formalism to improve on this, and link the spinor-helicity formalism to the chirality-flow formalism of papers I-IV. Finally, we comment on Berends-Giele recursions and how they can also be used to calculate scattering amplitudes efficiently.

In section 4 we focus on QCD, in particular focusing on calculations of its $su(N_c)$ gauge algebra. We describe how the colour and kinematics in any calculation are usually separated, and how to calculate the colour part. We then describe the expansion in the number of colours N_c used in paper V, and why it is useful. Additionally, we describe colour flow, which was the inspiration for the chirality-flow formalism developed in papers I-IV.

Section 5 describes the program MadGraph5_aMC@NLO, which is used in papers III and V to automate some of the scattering-amplitude optimisations described in this thesis. We provide an overview of the workflow of the program, describe how it calculates amplitudes, and say which parts of the program were updated in papers III and V.

Next, in section 6, we move from tree level to one-loop level. We describe one-loop integrals and their challenges, including divergences and how to regularise them, renormalisation, dimensional regularisation, the FDF formalism we built on in paper IV, and reducing tensor integrals.

We conclude and give an outlook in section 7. In section 8, all publications listed in this thesis are described in some detail, while in section 9, we list other work done during the


PhD which is not included here. Finally, after all of this, are the five papers of my thesis.

I A General Overview: Particle Physics, the Standard Model, and the Role of this Thesis within it

The goal of particle physics is extremely simple: to understand the most fundamental building blocks which make up all of the matter (i.e. stuff) in the universe. By ‘fundamental’ we mean that, starting from these basic pieces and the laws which describe how they interact with each other, we can describe everything in the world. Like many very simple questions, its complete answer is so complicated that we as a society have spent centuries of time and money trying to answer it. The goal of this thesis is to simplify one important tool used to find this complete answer.

First, let us discuss the size of these particles. Since we want the fundamental building blocks from which to create all other matter, we will necessarily be talking about small objects. In order to put into perspective just how small we really mean by ‘small’, we will start from the natural scale of our day-to-day lives of about 1m (or $\mathcal{O}(1\text{m})$ in scientific language), and zoom in until we are small enough to see the fundamental building blocks of nature.

If we zoom in on some everyday object, we will eventually reach the atoms which bind together to form it. These atoms are typically about $\mathcal{O}(1 \times 10^{-10}\text{m})$ long. For context, if we zoomed *out* by this much instead of zooming *in*, the combination of the Earth and our moon would only take up about the same amount of space in our view as a coin would on a table.

These atoms are not fundamental, since we know them to be made of protons, neutrons, and electrons. The protons and neutrons are, however, much smaller than the atom itself, with a size of $\mathcal{O}(1 \times 10^{-15}\text{m})$. If we instead zoomed out this much from our everyday scale of a metre, we would now comfortably fit the entire solar system into about $1/10^{\text{th}}$ of our field of view, taking up about the same space as a mobile phone would on a table. Nonetheless, these protons and neutrons are themselves made up of smaller objects called quarks and gluons, which, together with electrons, are the fundamental building blocks which make up our daily lives. 

We consider these fundamental particles to be completely point-like; that is, to take up a single point in space. To see them, it is easiest to smash together hydrogen nuclei (i.e. protons) or other atomic nuclei and try to measure the debris created. We then do our best

¹We are of course open to finding out that we are incorrect, and that these building blocks are themselves made up of even smaller and more fundamental things.

to ‘see’ which fundamental particles created the debris. To date, our best ‘microscope’ to do this is the Large Hadron Collider (LHC), which can probe physics occurring at about $\mathcal{O}(1 \times 10^{-19}\text{m})$. If we continue our visual of zooming out instead of in, we can now see all of our neighbouring stars, cannot see the Earth because it is far too small, and only need to zoom out 10 times more to also see the centre of the galaxy. That is, looking at these fundamental particles in our day-to-day lives requires a microscope of about the same power as one which would be used to find a football stadium in a picture of the entire Milky Way.

Now that we have reached the idea of pointlike particles as our fundamental building blocks, we instead ask how to define such a particle? That is, what is it about a quark that makes it a quark, and not an electron, or a photon, etc.? The answer, is that the world has several symmetries, and each symmetry gives each particle a measurable, unchanging property called an invariant. If we know the values of all of the different invariants of a given particle, we have fully defined the particle. One example of a symmetry is Lorentz symmetry, which says that physics should be invariant, that is, unchanged, under changes of speed or velocity (called boosts) and rotations. For example, physical processes do not care if we observe them by sitting still on Earth, or if we observe them while sitting on the international space station which is moving around the Earth. The physical process will be the same (though they may look quite different!) to both observers. Another important symmetry, called translation symmetry, is trivial, but profound. Translation symmetry says that physics will be unchanged if we move the entire universe a bit to the left (or of course, in any direction), and its consequences include that energy and momentum must be conserved. Indeed, combining Lorentz symmetry with translation symmetry, gives rise to the two invariants of a particle which play the starring role in this thesis, the mass and the spin of the particle, both of which can be separated into two categories with remarkably different properties.

For mass, we separate particles whose mass is zero, known as massless, from those which are massive (mass is non-zero). Massless particles always move at the speed of light, while massive ones can be stationary, and can never reach the speed of light. Even though only the photon and the gluon are truly massless, in many situations at the LHC, the particles move so fast that their mass is negligible, and we can approximate them to be massless. This is useful, because massless particles are far simpler to use in calculations than massive ones.

For spin, we separate *fermions*, defined as particles with half-integer-valued spin, i.e. $\frac{1}{2}$, $\frac{3}{2}$, etc., from *bosons*, which have integer-valued spin, i.e. 0, 1, etc. The spin is the minimal angular (rotational) momentum that a particle always has, is measured in units of Planck’s constant \hbar , and is called spin in analogy with an object spinning on its own axis but being

Standard Model of Elementary Particles

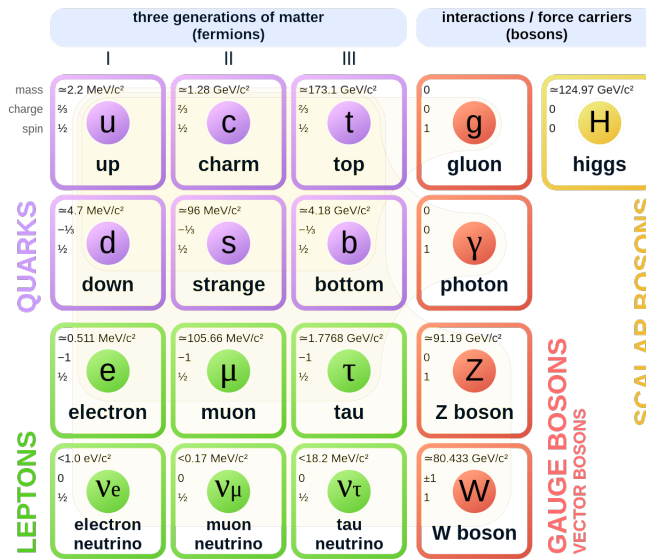


Figure 1: The Standard Model of particle physics. The fermions are separated into quarks (purple) which are colour charged, and leptons (green) which are not. The gauge bosons (red) mediate the different forces, while the Higgs (yellow) is responsible for giving each particle its mass. Figure from https://en.wikipedia.org/wiki/Standard_Model

otherwise still.² No fundamental particle has a spin larger than 2, and in this thesis we only consider particles with spin 0, $\frac{1}{2}$, and 1.

To the simplest approximation, the fermions (green and purple in figure 1) make up all of the atoms in the universe.³ The fermions interact with each other by exchanging gauge bosons (red in figure 1), which are said to mediate the different forces felt by the fermions. These forces exist because of a different set of symmetries called gauge symmetries. However, unlike Lorentz symmetry, they do not have a physically intuitive explanation. Nonetheless, there are three gauge symmetries about which we know, giving rise to the three forces of the Standard Model (SM) of particle physics. If a particle interacts through one of these forces, we say it is charged under that force. The charges and therefore behaviour of each particle under these forces, together with their mass and spin, leads to a

²However, this picture is in direct contradiction with the hypothesis that fundamental particles are point-like, an open paradox which is yet to be solved.

³Specifically, all of the atoms in the universe are made of only three fermions, up quarks, down quarks, and electrons.

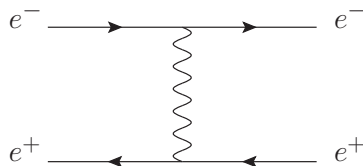


Figure 2: An example of a Feynman diagram describing an electron e^- and an anti-electron e^+ interacting with each other. The photon (wavy line) is considered the force carrier, and it is the exchange of this photon which means that the electron knows that the positron is there and vice versa.

full description of a particle. There are 17 such particles we know of today, and these are summarised in figure [1](#).

What are these three forces and how do they work? We start with the simplest force, quantum electrodynamics (QED), responsible for electromagnetism and most of our day-to-day experiences. All fermions except for the neutrinos are electrically charged and therefore interact under QED, and any such QED interaction occurs via the exchange of a *virtual* (i.e. not able to be measured) photon. Because of this, we say that the photon is the mediator of QED. QED interactions are most commonly described and calculated by using Feynman diagrams, which encode all of the quantum possibilities of going from an initial state to a final state. For example, by calculating the Feynman diagram in figure [2](#), we can calculate the probability of an electron moving close to an anti-electron, exchanging a photon, and therefore being attracted to the anti-electron. Such a diagram is at the heart of this thesis, whose first four papers describe a novel method to go from Feynman diagrams like this one to the probability of the scattering having occurred.

The second main force in the SM is the strong nuclear force (quantum chromodynamics, or QCD for short), and simplifying QCD calculations is the topic of paper V. Particles which are charged under the strong force are said to have colour charge, or just colour. There are three types of colour charge, called red, green, and blue, in analogy with the three primary colours of visible light.[3](#) To make something colour neutral in QCD, we can either combine a colour with its anti-colour (e.g. red with anti-red), or combine a red, green, and blue charge together, in analogy to adding red, green, and blue light together to create the neutral white light.

Similar to the way that electrically-charged objects have QED interactions, colour-charged objects have QCD interactions. Of the fermions, only the six quarks have colour charge, and their interactions are mediated by the exchange of a gluon. However, unlike the photon which is electrically neutral, the gluon is itself colour charged, so can interact with other

³Note that this has nothing to do with visible colours though, which come from QED and its photon.

gluons, meaning that gluons can and do exchange gluons with each other. This is an example of a non-abelian force, and the gluon self-interaction is what makes QCD extremely different to QED. For example, if you look at distances larger than the size of a proton ($\mathcal{O}(1 \times 10^{-15} \text{m})$), all objects will arrange themselves into colour-neutral objects called hadrons. Therefore, it is impossible to see bare quarks and gluons in our everyday lives, but instead we see them grouped together as hadrons, of which the most commonly known are the proton and neutron. On the other hand, at the energies and distances probed by the LHC, colour-charged objects act as if they are almost free from each other, and it is possible to distinguish (on average) the individual quarks and gluons rather than their colour-neutral hadrons. Therefore, at the distances probed in this thesis, we consider quarks and gluons as the individual particles, not the protons which we smashed together to create them, nor the sprays of hadrons which we directly measure at the detector.

The last force is the weak force, which is partially responsible for radioactive decay. All fermions are charged under the weak force, which is mediated by the W^\pm and Z bosons (note that the \pm in W^\pm implies that the W -bosons are electrically charged and undergo QED interactions). However, the weak force gives a problem, namely that the symmetry behind it is inconsistent with particles having a mass. To solve this problem, we introduce a scalar (i.e. spin-0) particle called the Higgs boson (yellow in figure 1), and use it to (spontaneously) break electroweak symmetry, which means that the interactions of the Higgs boson with other particles gives them a consistently defined mass⁵.

Now that we have described the standard model and said something about its interactions, it is worth describing how one confirms this picture of the world. Loosely speaking, at the LHC we smash together protons each with about 7 TeV of energy, and count how many particles are created together with their properties (energy, momenta, charges, etc.). The number N of observed collisions which have a certain set of properties is given by a very simple formula

$$N = \sigma L , \tag{1.1}$$

where L is the luminosity, i.e. an indication of how many protons we were able to put into our beam and therefore the amount of stuff which could in theory collide, while σ is the cross section, and gives the probability of colliding two protons and obtaining whatever final state you were looking for. The cross section is the square of the scattering amplitude integrated (think summed) over all possible energies and momenta that the final-state particles could have. The parameters of the integral itself are theory-independent (though they depend on the masses of the particles), while the scattering amplitude and its square are the stars of this thesis, are different for different particles and different theories, and therefore have to be recalculated for every process you are considering.

⁵Note that the gluon and the photon remain massless. Also, we do not yet know if the neutrinos get their very small masses in this way or in another way.

The original and most common way to calculate the scattering amplitude is to sum all possible Feynman diagrams for the process at hand. However, there are several ways to calculate and square a set of Feynman diagrams, i.e. to go from the pictures like figure 2, which represent some mathematical expression, to a set of numbers which can be integrated. The slowest method is the original method, for which every particle is unpolarised (does not have a specific spin direction). In this method, the scattering amplitude is a matrix, which has to be squared before laboriously taking its trace (summing the diagonal elements of the matrix). In the mid-1980s however, a new method was created called the spinor-helicity formalism. In the spinor-helicity formalism, each particle has a specific polarisation⁶, and after some matrix multiplication or algebra, the scattering amplitude is a complex number which can be squared easily. This made the spinor-helicity formalism ubiquitous in computer codes simulating particle collisions.

In the first four papers of this thesis, we developed chirality flow, which further simplifies the spinor-helicity formalism, and removes the need for most of the matrix multiplication or intermediate algebra. We did this for the full SM in the simplest, and next-to-simplest class of Feynman diagrams (called *tree-level* and *one loop* respectively). Additionally, we implemented the tree-level method for massless QED in the computer simulation program MadGraph5_aMC@NLO, allowing for predictions which were up to 10 times faster than before. Therefore, we are able to both create a conceptually simpler and clearer way to calculate Feynman diagrams, and to create a faster computer code to calculate scattering amplitudes and therefore cross sections.

Also, in paper V we explored a new implementation of QCD scattering amplitudes in MadGraph5_aMC@NLO. This implementation had two parts: first, it used a recursive algorithm called Berends-Giele recursion to bypass Feynman diagrams and calculate the scattering amplitude more efficiently; and second, it had a new implementation of the colour charge which was both able to improve the speed of a full QCD scattering amplitude, and was able to approximate the amplitude by only calculating part of the colour. This is important because the colour charge is the main bottleneck in QCD calculations in MadGraph5_aMC@NLO.

For those readers who are not physicists and have read this far, I would like to thank you for your effort and hope that this has enlightened you somewhat as to what this thesis is about. While I will try to start at the beginning, from the next section I will make a significant (quantum?) leap in expectations of my audience, and will assume a general physics background.

⁶The polarisation of a massless particles is its helicity, hence the name.

2 The fundamentals of Particle Physics

We now change from giving an overview, to giving specifics. In this section we will go over the fundamental physics underpinning particles and high-energy physics

2.1 The Lorentz Group, Mass, and Spin

For most of this thesis, the main symmetry group discussed is the Lorentz group and its associated little group, together with its conserved quantities of mass and spin/helicity. In this section we describe each of these objects in some detail.

The Lorentz group consists of all transformations of reference frame obtained by either changing your velocity or by rotating your coordinate system, with the change of velocity known as a boost. Restricting ourselves to the minimal required set of transformations (see e.g. [1, 2]), the Lorentz group is the special orthogonal group of rotations in three spatial and one time direction which preserves the direction of time, $SO(3, 1)_+$ (we can also think of boosts as a rotation between spatial and temporal coordinates). For simplicity of notation, we drop the $+$ and from now on understand that writing $SO(3, 1)$ means $SO(3, 1)_+$.

The Lorentz group is an example of a Lie group, which means that we can write a group element as an exponential of a *representation* of the group. Every object in the known universe transforms (i.e. changes its appearance) during a Lorentz transformation based upon which representation of the group it belongs to. For example, the most intuitive representation is the vector representation. A (four)vector, for example some position vector $x^\mu = (t, x, y, z)$, will transform into $x'^\mu = (t', x', y', z')$ based on the equation

$$x^\mu \rightarrow x'^\mu = \Lambda^\mu_\nu x^\nu, \quad (2.1)$$

where $\mu, \nu = 0, 1, 2, 3$ are Lorentz indices, Λ^μ_ν depends on the transformation at hand, and all repeated indices in this thesis are summed over unless otherwise stated. For example, for a rotation by an angle θ around the z -axis and a boost by speed v along the z -axis we have

$$\Lambda^\mu_\nu \stackrel{\text{rot}}{=} \begin{pmatrix} 1 & 0 & 0 & 0 \\ 0 & \cos \theta & -\sin \theta & 0 \\ 0 & \sin \theta & \cos \theta & 0 \\ 0 & 0 & 0 & 1 \end{pmatrix}, \quad \Lambda^\mu_\nu \stackrel{\text{boost}}{=} \begin{pmatrix} \gamma & 0 & 0 & -v\gamma \\ 0 & 1 & 0 & 0 \\ 0 & 0 & 1 & 0 \\ -v\gamma & 0 & 0 & \gamma \end{pmatrix}, \quad (2.2)$$

where $\gamma = 1/\sqrt{1 - v^2}$, and we use natural units in which the speed of light and Planck's constant are equal to one.

It is very useful to think of infinitesimal transformations, writing the transformation as doing nothing plus doing something incredibly small,

$$\Lambda^\mu_\nu = \delta^\mu_\nu - \frac{i}{2} (\omega_{\rho\sigma} J^{\rho\sigma})^\mu_\nu + \mathcal{O}(\omega^2) , \quad (2.3)$$

where we introduce a small parameter $\omega_{\mu\nu} = -\omega_{\nu\mu}$ and the generators of the group $J^{\mu\nu} = -J^{\nu\mu}$. The exact form of the generators of the group depends on the representation which is being considered. In our example above, the generators of rotations (boosts) around (along) the z -axis can be found by taking the rotation angle (boost speed) very small and placing its value into $\omega_{\rho\sigma}$, and then subtracting unity:

$$J^\mu_\nu \stackrel{\text{rot}}{=} i \begin{pmatrix} 0 & 0 & 0 & 0 \\ 0 & 0 & -1 & 0 \\ 0 & 1 & 0 & 0 \\ 0 & 0 & 0 & 0 \end{pmatrix} , \quad J^\mu_\nu \stackrel{\text{boost}}{=} i \begin{pmatrix} 0 & 0 & 0 & -1 \\ 0 & 0 & 0 & 0 \\ 0 & 0 & 0 & 0 \\ -1 & 0 & 0 & 0 \end{pmatrix} . \quad (2.4)$$

Using that in this representation we have 4×4 matrices and that $J^{\mu\nu} = -J^{\nu\mu}$, we conclude that there are six independent generators of the Lorentz group, three for the boosts along the x, y , and z axes, labelled K_i for $i = x, y, z = 1, 2, 3$, and three for rotations around those three axes, labelled J_i .

Regardless of the representation of the group, these six generators obey the Lie algebra

$$[J_i, J_j] = i\epsilon_{ijk} J_k , \quad [J_i, K_j] = i\epsilon_{ijk} K_k , \quad [K_i, K_j] = -i\epsilon_{ijk} J_k , \quad (2.5)$$

where we introduce the commutator $[A, B] \equiv AB - BA$ and the totally antisymmetric Levi-Cevita tensor ϵ_{ijk} .

A key realisation which is utilised repeatedly in this thesis, is to recast the generators of the Lorentz algebra into two independent sets of generators, $N_i^{L/R}$, by using

$$\textcolor{blue}{N}_i^L = \frac{1}{2} (J_i - iK_i) , \quad \textcolor{red}{N}_i^R = \frac{1}{2} (J_i + iK_i) , \quad (2.6)$$

which have the Lie algebra relations

$$[\textcolor{blue}{N}_i^L, \textcolor{blue}{N}_j^L] = i\epsilon_{ijk} \textcolor{blue}{N}_k^L , \quad [\textcolor{red}{N}_i^R, \textcolor{red}{N}_j^R] = i\epsilon_{ijk} \textcolor{red}{N}_k^R , \quad [\textcolor{blue}{N}_i^L, \textcolor{red}{N}_j^R] = 0 . \quad (2.7)$$

Here, the first two relations say that both $\textcolor{blue}{N}^L$ and $\textcolor{red}{N}^R$ obey the $su(2)$ algebra⁷ and the last relation states that the two algebras are independent of each other. We have therefore shown the equivalence of the Lorentz algebra and two copies of $su(2)$, one called the **left $su(2)$** , the other called the **right $su(2)$** , and we classify particles based upon their representation $(\textcolor{blue}{j}_L, \textcolor{red}{j}_R)$ of the two $su(2)$ s:

⁷Groups are written with capital letters, and their algebras are written with lower-case letters.

- $(0, 0)$ are scalar particles
- $(\frac{1}{2}, 0)$ are **left**-chiral, two-component Weyl spinors
- $(0, \frac{1}{2})$ are **right**-chiral, two-component Weyl spinors
- $(\frac{1}{2}, 0) \oplus (0, \frac{1}{2})$ are four-component Dirac spinors
- $(\frac{1}{2}, \frac{1}{2})$ are vector particles.

Note that even though we have described the algebra of $su(2)$, the Lorentz group is not related to the $SU(2)$ group. It is instead given by two copies of the group $SL(2, \mathbb{C})$, whose algebra $sl(2, \mathbb{C})$ coincides with the algebra $su(2)$.

Another key aspect of any group and its algebra are its invariants; that is, the quantities which are unchanged when doing a group transformation.

In the vector representation of the Lorentz group, arguably the most important invariants are the metric and the scalar product which it creates. The metric defines what we mean by the distance between two objects, and in the vector representation we have

$$x^2 \equiv g_{\mu\nu} x^\mu x^\nu = t^2 - x^2 - y^2 - z^2, \quad g_{\mu\nu} = \text{diag}(1, -1, -1, -1), \quad (2.8)$$

where $g_{\mu\nu}$ is the metric and both the metric and x^2 will not change during a Lorentz transformation. Switching to momentum-space, the invariant of a momentum with itself is the square of its mass, m^2 , defined as

$$m^2 = p^2 = g_{\mu\nu} p^\mu p^\nu = E^2 - p_x^2 - p_y^2 - p_z^2. \quad (2.9)$$

As discussed in section [1](#), in this thesis we want to distinguish two cases: either the mass of a particle vanishes (massless) or it does not (massive). As we will see in the next section, this distinction leads to different spin quantum numbers and therefore different behaviours of a particle.

2.1.1 Wigner's little group

One way to understand the spin quantum numbers of the Lorentz group is by using a soon-to-be-described definition of a one-particle state, and looking at the action of Wigner's little group on that state [1–4]. We extend the Lorentz group to the Poincaré group by adding translations of spacetime which are generated by the momentum operator⁸ P , whose eigenvalue on a state is its momentum p . We use the Dirac ket $|p, \sigma\rangle$ to describe a state of momentum p and other Poincaré degrees of freedom σ ; that is

$$P^\mu |p, \sigma\rangle = p^\mu |p, \sigma\rangle. \quad (2.10)$$

⁸We will sometimes write fourvectors without their vector index for brevity.

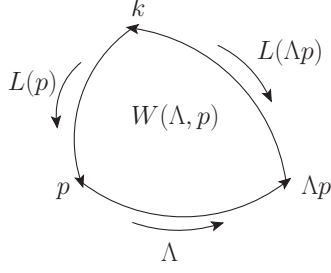


Figure 3: Visualising a Wigner rotation. The particle is transformed from the standard momentum k to the observed momentum p , transformed by Λ to Λp , and then transformed back to the standard momentum k .

The goal now is to understand what the σ degree(s) of freedom can be. To do this, we start by rewriting our state of arbitrary momentum p as a Lorentz-transformed state from some standard momentum k ,

$$|p, \sigma\rangle \sim U(L[p])|k, \sigma\rangle, \quad (2.11)$$

where we ignore the overall normalisation since it does not affect our discussion. Here, $L[p]$ is some Lorentz transformation which takes you from the standard momentum k to the arbitrary momentum p , and $U(L[p])$ is that transformation written in the representation of the particle $|k, \sigma\rangle$. By definition, this boost does not change the σ degree(s) of freedom.

An obvious question is, what is this standard momentum k ? Since a Lorentz transformation cannot change the mass of a particle, nor flip the sign of its energy (see section 2.1), we need a different k for both massless and massive particles, and need a different k for positive- and negative-energy particles (and a further k for the vacuum). In this thesis, we only need to understand the difference between massless and massive particles, and take positive energy for both simplicity and physical reality. We therefore have

- Massless particles: $k^\mu = (\omega, 0, 0, \omega)$. Massless particles are always moving, so we parameterise them to move along the z -axis with some energy ω .
- Massive particles: $k^\mu = (m, 0, 0, 0)$. For massive particles, we choose the standard momentum to equal the rest-frame momentum.

Now that we have the standard momentum, the question is how to understand σ ? To answer this, we act with an arbitrary Lorentz transformation Λ on the state $|p, \sigma\rangle$, multiply

by one, then use $U(\Lambda)U(\Lambda') = U(\Lambda\Lambda')$, which holds for any representation:

$$\begin{aligned} U(\Lambda)|p, \sigma\rangle &\sim U(\Lambda)U(L[p])|k, \sigma\rangle = \underbrace{U(L[\Lambda p])U(L^{-1}[\Lambda p])}_1 U(\Lambda L[p])|k, \sigma\rangle \\ &= U(L[\Lambda p])U(\underbrace{L^{-1}[\Lambda p]\Lambda L[p]}_{W(\Lambda, p)})|k, \sigma\rangle, \end{aligned} \quad (2.12)$$

where in the last underbrace we introduce the Wigner rotation

$$W(\Lambda, p) = L^{-1}[\Lambda p]U(\Lambda L[p]), \quad (2.13)$$

which does not change the standard momentum k (see figure 3 for an intuitive picture of this rotation). Therefore, we have

$$U(W(\Lambda, p))|k, \sigma\rangle = \sum_{\sigma, \sigma'} C_{\sigma, \sigma'}|k, \sigma'\rangle, \quad (2.14)$$

that is, that the Wigner rotation does not change the momentum, but may change σ , transforming the state σ to a linear combination of states with σ' .

The full effect of boosting the state is then

$$\begin{aligned} U(\Lambda)|p, \sigma\rangle &\sim U(L[\Lambda p])U(W(\Lambda, p))|k, \sigma\rangle = \sum_{\sigma, \sigma'} C_{\sigma \sigma'} U(L[\Lambda p])|k, \sigma'\rangle \\ &\sim \sum_{\sigma, \sigma'} C_{\sigma \sigma'} |\Lambda p, \sigma'\rangle, \end{aligned} \quad (2.15)$$

where we again ignore normalisation factors. Eq. (2.15) says that to boost a particle we first go back to the standard momentum, Wigner rotate and possibly change its σ values, and then we boost to the new momentum without changing σ .

These Wigner rotations define what is called the little group, and in turn this defines the spin quantum numbers σ of a particle. We now look at the two different little groups, one for massless particles, the other for massive ones.

Massless

We begin with the massless little group, and try to find the generators of all of its transformations. To do so, we consider an infinitesimal transformation $\Lambda^\mu_\nu = \delta^\mu_\nu - i\omega^\mu_\nu$, then use the metric to lower the upper index to get $\Lambda_{\mu\nu} = g_{\mu\nu} - i\omega_{\mu\nu}$ (this allows us to use that $\omega_{\mu\nu} = -\omega_{\nu\mu}$). The effect of the transformation on k is

$$\omega_{\mu\nu}k^\nu = \begin{pmatrix} 0 & \omega_{01} & \omega_{02} & \omega_{03} \\ -\omega_{01} & 0 & \omega_{12} & \omega_{13} \\ -\omega_{02} & -\omega_{12} & 0 & \omega_{23} \\ -\omega_{03} & -\omega_{13} & -\omega_{23} & 0 \end{pmatrix} \begin{pmatrix} \omega \\ 0 \\ 0 \\ \omega \end{pmatrix} = 0, \quad (2.16)$$

with solution

$$\omega_{\mu\nu} = i \begin{pmatrix} 0 & \alpha & \beta & 0 \\ -\alpha & 0 & \theta & \alpha \\ -\beta & -\theta & 0 & \beta \\ 0 & -\alpha & -\beta & 0 \end{pmatrix} = \alpha(K_1 + J_2)_{\mu\nu} + \beta(K_2 - J_1)_{\mu\nu} + \theta(J_3)_{\mu\nu} , \quad (2.17)$$

where J_i and K_j are the generators of Lorentz transformations from before.

Interestingly, if α and β are non-zero, then θ becomes a continuous variable (see e.g. [1, 2]), and we do not know of any massless particles with continuous spin.⁸ Therefore, we restrict ourselves to the case $\alpha = \beta = 0$, and the little group is restricted to $O(2) \cong U(1)$, which has a single eigenvalue, the (quantised) spin along the direction of motion, i.e. the helicity.

We therefore conclude that the generator of the Wigner rotation is the helicity operator, and that, in the absence of other symmetry groups such as gauge symmetries, all physical massless particles can be described by their two properties, their momentum and their helicity $\sigma \equiv h$. Note that this implies that a massless particle of any total spin j has only two spin degrees of freedom $h = \pm j$, often just written as $h = \pm$.

Massive

Massive particles are more straightforward than massless ones. In this case, the Wigner rotations are any rotation in space, the little group is $SO(3) \cong SU(2)$, and the σ eigenvalues are the total spin of the particle j and its projection J_s along some direction s , with values $J_s = -j, -j+1, \dots, j$. Therefore, a massive particle can have $2J_s + 1$ values for its spin eigenvalue, and is fundamentally different to a massless particle.

2.2 Lagrangians

Now that we understand a bit more about symmetry groups, in particular the Lorentz group, we briefly describe Lagrangians, which encode the physics of a given theory. The Lagrangian (more properly the Lagrangian density) is the kinetic energy minus the potential energy of a field, and involves all possible combinations of the fields which correctly obey the symmetries imposed. For example, all Lagrangians are required to be invariant under Lorentz symmetry, so the Lagrangian of a scalar field with no further symmetries or requirements imposed is

$$\mathcal{L} = \frac{1}{2} (\partial_\mu \phi) (\partial^\mu \phi) - \frac{m^2}{2} \phi^2 - \frac{\lambda_3}{3!} \phi^3 - \frac{\lambda_4}{4!} \phi^4 - \dots , \quad (2.18)$$

⁸There have, however, been several papers describing the properties of such hypothetical, continuous spin particles, e.g. [5–8].

where ϕ is the scalar field, m the mass of the scalar, λ_3, λ_4 are couplings, the term with the derivatives is the kinetic energy, and all terms with a minus sign are the potential energy.

In addition to the Lagrangian, another key concept in physics is the action S , defined as the integral of the Lagrangian

$$S \equiv \int d^4x \mathcal{L}(\phi(x), \partial_\mu \phi(x)) , \quad (2.19)$$

where we made the x dependence of the field ϕ explicit. The principle of least action states that the stationary points of the action, $\delta S = 0$, describe how a field evolves from one state to another. Therefore, we obtain the equations of motion of the field using $\delta S = 0$, which gives the Euler-Lagrange equations

$$\partial_\mu \left(\frac{\partial \mathcal{L}}{\partial (\partial_\mu \phi)} \right) - \frac{\partial \mathcal{L}}{\partial \phi} = 0 , \quad (2.20)$$

where in general we have one such equation for each field ϕ within the Lagrangian.

We pause to make several remarks. First, we note that the action must be dimensionless. Counting dimensions of energy, the Lagrangian itself must have dimension 4, and therefore the fields ϕ and coupling λ_3 both have dimension 1, while the four-point coupling λ_4 is dimensionless. This will be important when we look at loop integrals and dimensional regularisation in section [6.2](#).

Second, in the Standard Model, the Lagrangian must be invariant under not only Lorentz symmetry, but also the Standard Model gauge groups $SU(3)_C \times SU(2)_L \times U(1)_Y$. However, the actual form of this Lagrangian is unimportant for this thesis so is not written here.^{[19](#)}

Finally, the Lagrangian is extremely important in scattering amplitudes, since one is able to derive all of the rules necessary for calculating scattering amplitudes from the Lagrangian. Such rules are called the Feynman rules, and are used ubiquitously in this thesis. However, we will not discuss here how to move from the Lagrangian to Feynman rules, and instead point to e.g. [\[1, 2, 9, 10\]](#).

2.3 Particle Wavefunctions

A crucial part of this thesis is correctly describing the wavefunctions of particles of a given spin or helicity. Therefore, we will give a brief overview of the components necessary for this thesis, but more information can be found in e.g. [\[1, 2, 9–12\]](#).

¹⁹The interested reader can find this Lagrangian in many forms, from the very compact but possibly uninformative form often written on mugs or t-shirts, to the more complete form written in textbooks such as [\[1, 2, 9, 10\]](#).

In the chirality-flow formalism which comprises the majority of this thesis, we simplify the part of a scattering amplitude calculation which is derived from the spins of the particles. Our method describes particles of spin 0, $\frac{1}{2}$, and 1, but since scalar particles have spin 0, their spin-structure is trivial and there is little to say about them.

The first non-trivial particles with regard to spin are the spinors, which have spin $\frac{1}{2}$ and obey the famous Dirac equations. There are two types of spinors: particles of spin J_s , whose momentum-space wavefunction is denoted by $u^{J_s}(p)$; and antiparticles of spin J_s , with momentum-space wavefunction $v^{J_s}(p)$. Each of these spinors obeys a slightly different Dirac equation

$$\begin{aligned} (\not{p} - m)u^{J_s}(p) &= 0, & \bar{u}^{J_s}(p)(\not{p} - m) &= 0, \\ (\not{p} + m)v^{J_s}(p) &= 0, & \bar{v}^{J_s}(p)(\not{p} + m) &= 0, \end{aligned} \quad (2.21)$$

where we introduced the Feynman slash $\not{p} \equiv p_\mu \gamma^\mu$, the Dirac-conjugated wavefunctions $\bar{u}^{J_s}(p) \equiv (u^{J_s})^\dagger(p)\gamma^0$ and $\bar{v}^{J_s}(p) \equiv (v^{J_s})^\dagger(p)\gamma^0$, and the Dirac gamma matrices γ^μ , defined as obeying the Clifford algebra

$$\{\gamma^\mu, \gamma^\nu\} \equiv \gamma^\mu \gamma^\nu + \gamma^\nu \gamma^\mu = 2g^{\mu\nu}. \quad (2.22)$$

In this thesis, the four-dimensional Clifford algebra, eq. (2.22), is realised using the Weyl, or chiral, basis

$$\gamma^\mu = \begin{pmatrix} 0 & \sigma^\mu \\ \bar{\sigma}^\mu & 0 \end{pmatrix}, \quad \sigma^\mu = (1, \vec{\sigma}), \quad \bar{\sigma}^\mu = (1, -\vec{\sigma}), \quad (2.23)$$

where $\vec{\sigma}$ is a vector of the three Pauli matrices

$$\sigma^1 = \begin{pmatrix} 0 & 1 \\ 1 & 0 \end{pmatrix}, \quad \sigma^2 = \begin{pmatrix} 0 & -i \\ i & 0 \end{pmatrix}, \quad \sigma^3 = \begin{pmatrix} 1 & 0 \\ 0 & -1 \end{pmatrix}. \quad (2.24)$$

In addition to the four γ -matrices, it is convenient to introduce a fifth γ -matrix, γ^5 , obeying

$$\gamma^5 = i\gamma^0\gamma^1\gamma^2\gamma^3, \quad (\gamma^5)^2 = 1, \quad (\gamma^5)^\dagger = \gamma^5, \quad \gamma^5 = \begin{pmatrix} -1 & 0 \\ 0 & 1 \end{pmatrix}, \quad (2.25)$$

where the matrix representation is only true in the chiral basis, but other relations are basis independent. γ^5 can be used to create the chiral projection operators

$$\begin{aligned} P_{R/L} &= \frac{1 \pm \gamma^5}{2}, & P_R + P_L &= 1, \\ P_R P_L &= 0, & P_R P_R &= P_R, & P_L P_L &= P_L, \end{aligned} \quad (2.26)$$

¹¹By using spin J_s we implicitly imply that these spinors are massive. For a discussion of massless spinors see below.

which allow us to separate the **left-chiral** part of a spinor, transforming under the $(\frac{1}{2}, 0)$ representation of the Lorentz group, from the **right-chiral** part of a spinor, transforming under the $(0, \frac{1}{2})$ representation of the Lorentz group (see eq. (2.7) and the discussion below it). Using that $1 = P_L + P_R$, we explicitly see that a Dirac spinor is simply a sum of both a **left-** and a **right-chiral** Weyl spinor, i.e. that Dirac spinors transform under the $(\frac{1}{2}, 0) \oplus (0, \frac{1}{2})$ representation of the Lorentz group.

It is useful to use different symbols to distinguish a **left-chiral** spinor from a **right-chiral** one. Specifically, we use **square** bras and kets to denote **left-chiral**, two-component, Weyl spinors, and **angled** bras and kets to denote **right-chiral**, two-component, Weyl spinors, writing

$$\begin{aligned} u^{J_s}(p) &= \begin{pmatrix} |p_1] \\ |p_2\rangle \end{pmatrix}, & v^{J_s}(p) &= \begin{pmatrix} |p'_1] \\ |p'_2\rangle \end{pmatrix}, \\ \bar{u}^{J_s}(p) &= ([p_2| \langle p_1|), & \bar{v}^{J_s}(p) &= ([p'_2| \langle p'_1|), \end{aligned} \quad (2.27)$$

where the momenta p_1 and p_2 may be different to p'_1 and p'_2 and are, for now, left undefined (see section 3.2 and paper II for their definitions). These two-component spinors will be used copiously in the first four papers of this thesis.

An important property of Dirac spinors is their spin sums

$$\sum_{J_s} u^{J_s}(p) \bar{u}^{J_s}(p) = \not{p} + m, \quad \sum_{J_s} v^{J_s}(p) \bar{v}^{J_s}(p) = \not{p} - m, \quad (2.28)$$

which are required in traditional Feynman-diagram calculations.

Finally for spinors, we comment that when $m = 0$ the u and v spinors both have the same Dirac equation and the same spin sum. It can be shown that either the **square** or **angle** spinor vanishes in this case, such that the four-component Dirac spinor instead becomes a two-component **left-** or **right-chiral** Weyl spinor, and that we have

$$u^h(p) = v^{-h}(p), \quad \bar{u}^h(p) = \bar{v}^{-h}(p), \quad (2.29)$$

where we changed the massive spin quantum number J_s to the massless one, the helicity h .

Next, we consider spin-1 particles. For this thesis, it is sufficient to know that spin-1 wavefunctions involve a polarisation vector $\epsilon_s^\mu(p)$ of some spin s obeying

$$\epsilon_s(p) \cdot \epsilon_{s'}^*(p) = -\delta_{ss'}, \quad p \cdot \epsilon_s(p) = 0, \quad (2.30)$$

where we use the notation $A \cdot B \equiv A^\mu B_\mu$ for the first time. This equation gives the normalisation of the polarisation vectors, as well as the transversality condition, and is valid for both massive particles ($s \equiv J_s$) and massless ones ($s \equiv h$).

2.4 Gauge Fixing

In the previous section we saw the wavefunctions which describe the external particles of Feynman diagrams and scattering processes. In this section, we will instead describe the propagators of internal spin-1 particles. We will implicitly assume an abelian gauge symmetry like QED for simplicity, but, unless otherwise stated, our conclusions will hold in non-abelian theories like QCD as well.

The massless spin-1 gauge bosons in the Standard Model obey gauge symmetry, which says that physics is invariant under the following transformation of their fields A_μ :¹²

$$A_\mu \rightarrow A_\mu(x) + \partial_\mu \alpha(x) , \quad (2.31)$$

where $\alpha(x)$ is an arbitrary scalar function. Eq. (2.31) implies that there is a continuously infinite number of physically equivalent fields, and therefore the propagator is ill defined. Arguably the most common solution to this, is to explicitly break gauge symmetry by adding a gauge-fixing term to the Lagrangian [14],¹³

$$\mathcal{L}_{\text{gf}} = -\frac{1}{\xi^2} (\partial_\mu A^\mu)^2 , \quad (2.32)$$

which ensures that there is exactly one A field per physical field. Here, ξ is a free parameter which helps define the choice of gauge, and this choice of gauge fixing is called the R_ξ gauge. The parameter ξ , like any gauge parameter, will show up as an artefact in intermediate stages of a calculation, however all physical quantities must eventually be gauge invariant and therefore independent of the choice of ξ .

Having now fixed the gauge, the spin-1 propagator is well defined, and has the form

$$\mu \sim \text{wavy line} \sim \nu \quad \sim -\frac{i}{p^2} \left(g_{\mu\nu} - (1 - \xi) \frac{p_\mu p_\nu}{p^2} \right) , \quad (2.33)$$

which is simplified by choosing $\xi = 1$. Such a choice is called Feynman or Feynman-’t Hooft gauge, and is used almost exclusively in this thesis.

3 Scattering Amplitudes and How to Calculate Them

As was discussed around eq. (1.1), at any collider experiment we count events and use them to measure the cross section, i.e. the probability that such an event occurs. In this section

¹²For a non-abelian symmetry, we should add an extra term to the gauge transformation, eq. (2.31) [13].

¹³If the theory is non-abelian, this choice will also require the addition of non-commuting scalar particles called ghosts to the Lagrangian.

we first relate this cross section to scattering amplitudes, the overarching topic of this thesis, and then describe the spinor-helicity formalism on which papers I-IV and the chirality-flow formalism are based. Finally, we discuss Berends-Giele recursions and how they bypass Feynman diagrams.

The partonic cross section¹⁴ $\hat{\sigma}$ for a $2 \rightarrow n$ scattering process involving SM particles is calculated using [17–19]

$$\hat{\sigma} = \frac{1}{4F} \frac{1}{2\pi^{3n-4}} \int \prod_{i=1}^n \frac{d^3 p_i}{2E_i} \delta^4(p_{in} - p_{out}) |\overline{M(a+b \rightarrow n)}|^2, \quad (3.1)$$

where $F = \sqrt{(p_a \cdot p_b)^2 - m_a^2 m_b^2}$ is called the Møller flux, the product runs over all n final-state particles i , the Dirac delta function ensures momentum conservation, we integrate over all possible momenta of the final-state particles, and $M(a+b \rightarrow n)$ is the scattering amplitude for the process $a+b \rightarrow n$ and is usually summed and averaged over polarisations and colours (hence the bar). Note that we will use the words scattering amplitude, amplitude, and matrix element interchangeably.

In the electroweak theory, and in QCD at energies much higher than 1 GeV, the couplings involved are small, allowing a perturbative expansion of the cross section in the number of powers of the coupling (see e.g. [10, 15–17])

$$\hat{\sigma} = \hat{\sigma}^{\text{LO}} + \alpha \hat{\sigma}^{\text{NLO}} + \alpha^2 \hat{\sigma}^{\text{NNLO}} + \dots, \quad (3.2)$$

where we have called a generic (squared) coupling α , and made use of the short-hand notation LO for leading order, NLO for next-to-leading order, etc. Each $\hat{\sigma}^i$ is individually calculated using eq. (3.1), and the scattering amplitudes need to be calculated separately at each order of the perturbative expansion.

It is now that we turn to the main object of this thesis, the scattering amplitude. This is typically calculated by summing Feynman diagrams,¹⁵ which encode all of the ways we can go from some initial particles to some final particles, and give some mathematical expression used to calculate the amplitude. For example, using the Feynman rules in paper I, there is only one possible LO Feynman diagram for the process $e^+e^- \rightarrow \mu^+\mu^-$, and therefore its

¹⁴The hat here is to distinguish the partonic cross section from the hadronic cross section. A discussion of the difference between them and their relation to each other is outside the scope of this thesis. If interested, see e.g. [15–17].

¹⁵Note that it is also now common to use off- and on-shell recursion relations which alleviate several problems of Feynman diagrams, especially the scaling with the particle multiplicity. See section 3.3 and e.g. [11, 12, 20–23] for more.

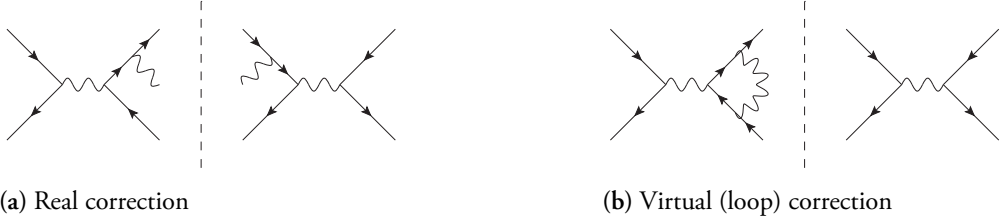


Figure 4: Two examples of contributions to an NLO cross section. For both examples, the left-hand-side represents the amplitude, while the right-hand side represents the conjugate amplitude. In (a) the NLO contribution is at tree level, while in (b) we have a loop-level contribution.

amplitude is given by that diagram:

$$\begin{aligned}
 M(e^+e^- \rightarrow \mu^+\mu^-) &= \\
 &= ie^2 \frac{[\bar{v}_{s_1}(1)\gamma^\mu u_{s_2}(2)] [\bar{u}_{s_4}(4)\gamma_\mu v_{s_3}(3)]}{(p_1 + p_2)^2}, \quad (3.3)
 \end{aligned}$$

where e is the electromagnetic coupling, the spinors u, \bar{u}, v, \bar{v} and gamma matrices γ^μ are defined in section 2.3, and we have introduced the shorthand notation $i \equiv p_i$. For simplicity, we use Feynman gauge (see section 2.4). How to square the right-hand-side of eq. (3.3) to get a probability will be explained in sections 3.1 and 3.2. For now, we comment that the factor $ie^2/(p_1 + p_2)^2$ is trivial to calculate, but the factor $[\bar{v}(1)\gamma^\mu u(2)] [\bar{u}(4)\gamma_\mu v(3)]$ coming from the spin structure requires some effort. In the next few sections, and in the first four papers of this thesis, we will mainly focus on calculating and simplifying this spin structure.

Finally, we note that Feynman diagrams can in general have a tree-like structure as in eq. (3.3) (called a tree-level diagram), or a loop-like structure (called a loop diagram). An example of each is given in figure 4. Tree-level diagrams are far simpler to calculate than loop diagrams, because the momentum of every particle involved is determined. In loop diagrams, there is at least one unconstrained momentum which has to be integrated over, often yielding infinite results (see section 5).

3.1 Textbook method to Calculate a Scattering Amplitude

Now we are ready to show how to calculate the squared scattering amplitude. The textbook method to do this (see e.g. [10]) is to square the right-hand-side of eq. (3.3), sum over spins,

then use the cyclicity of a trace and the spin-sum rules in eq. (2.28) to obtain

$$\begin{aligned}
 \left| \begin{array}{c} e^-(2) \\ e^+(1) \end{array} \right. & \left. \begin{array}{c} \mu^+(3) \\ \mu^-(4) \end{array} \right|^2 = \frac{e^4}{(p_1 + p_2)^4} \sum_{s_1, s_2, s_3, s_4} [\bar{v}_{s_1}(1) \gamma^\mu u_{s_2}(2)] [\bar{u}_{s_4}(4) \gamma_\mu v_{s_3}(3)] \\
 & \times [\bar{u}_{s_2}(2) \gamma^\nu v_{s_1}(1)] [\bar{v}_{s_3}(3) \gamma_\nu u_{s_4}(4)] \\
 & = \frac{e^4}{(p_1 + p_2)^4} \sum_{s_1, s_2, s_3, s_4} \text{Tr} [v_{s_1}(1) \bar{v}_{s_1}(1) \gamma^\mu u_{s_2}(2) \bar{u}_{s_2}(2) \gamma^\nu] \\
 & \times \text{Tr} [u_{s_4}(4) \bar{u}_{s_4}(4) \gamma_\mu v_{s_3}(3) \bar{v}_{s_3}(3) \gamma_\nu] \\
 & = \frac{e^4}{(p_1 + p_2)^4} \text{Tr} [\not{1} - m_1) \gamma^\mu (\not{2} + m_2) \gamma^\nu] \\
 & \times \text{Tr} [\not{4} + m_4) \gamma_\mu (\not{3} - m_3) \gamma_\nu] , \quad (3.4)
 \end{aligned}$$

where s_i is the spin of particle i . To write this as a complex number which can be integrated over, we need to use the known relations for traces of gamma matrices, e.g.

$$\begin{aligned}
 \text{Tr} [\gamma^{\mu_1} \gamma^{\mu_2}] &= 4g^{\mu_1 \mu_2} , \quad \text{Tr} [\gamma^{\mu_1} \dots \gamma^{\mu_{2n+1}}] = 0 , \\
 \text{Tr} [\gamma^{\mu_1} \dots \gamma^{\mu_4}] &= 4(g^{\mu_1 \mu_2} g^{\mu_3 \mu_4} - g^{\mu_1 \mu_3} g^{\mu_2 \mu_4} + g^{\mu_1 \mu_4} g^{\mu_2 \mu_3}) . \quad (3.5)
 \end{aligned}$$

To simplify the calculation, we will assume that all particles are massless, meaning that

$$\begin{aligned}
 \left| \begin{array}{c} e^-(2) \\ e^+(1) \end{array} \right. & \left. \begin{array}{c} \mu^+(3) \\ \mu^-(4) \end{array} \right|^2 = \frac{e^4}{(p_1 + p_2)^4} \text{Tr} [\not{1} \gamma^\mu \not{2} \gamma^\nu] \text{Tr} [\not{4} \gamma_\mu \not{3} \gamma_\nu] \\
 & = \frac{16e^4}{(p_1 + p_2)^4} [1^\mu 2^\nu - (p_1 \cdot p_2) g^{\mu\nu} + 1^\nu 2^\mu] \\
 & \quad \times [4_\mu 3_\nu - (p_3 \cdot p_4) g_{\mu\nu} + 4_\nu 3_\mu] \\
 & = \frac{8e^4}{s_{12}^2} \left[s_{14} s_{23} + s_{13} s_{24} + \frac{1}{2} s_{12} s_{34} (g_\mu^\mu - 4) \right] , \quad (3.6)
 \end{aligned}$$

where we used that $g^{\mu\nu} g_{\mu\nu} = g_\mu^\mu$, and introduced the notation $s_{ij} \equiv (p_i + p_j)^2$ which for massless momenta simplifies to $s_{ij} = 2p_i \cdot p_j$. The trace of the metric g_μ^μ is equal to the number of dimensions of spacetime, so in this case, $g_\mu^\mu = 4$ and the last term disappears, giving

$$\left| \begin{array}{c} e^-(2) \\ e^+(1) \end{array} \right. \left. \begin{array}{c} \mu^+(3) \\ \mu^-(4) \end{array} \right|^2 = \frac{8e^4}{s_{12}^2} [s_{14} s_{23} + s_{13} s_{24}] , \quad (3.7)$$

for the squared scattering amplitude $\left| \overline{M(e^+e^- \rightarrow \mu^+\mu^-)} \right|^2$.

At this point we pause to make a few comments. Firstly, this was the simplest non-trivial process we can calculate, yet still took about a page of abridged algebra. More difficult processes quickly become intractable without the use of a computer, and even with a computer this method is very inefficient.

Secondly, since the square of the amplitude gives momentum invariants, the amplitudes themselves should be some sort of square root of these invariants. This will be realised in the spinor-helicity method in the next section. However, in this method the amplitude was a matrix, hence it was difficult to square and complete the calculation.

Finally, in four dimensions, the momentum invariants s_{ij} we obtain at the end only involve contractions of momenta from different fermion lines. It is as if the spin structure gives a momentum which flows through the photon from one fermion line to another, an observation which the chirality-flow method of this thesis makes very obvious and transparent.

3.2 The Spinor-Helicity Formalism

One way to improve this calculation is by using the spinor-helicity formalism [11, 12, 24–40]. In this formalism, every particle is given a specific value of its spin quantum number (cf. section 2.1.1). Importantly, this allows the amplitude to be written in terms of complex numbers, rather than a matrix, making it easier to square and quicker to calculate on a computer. Further, the chirality-flow method of this thesis is a simplification of the spinor-helicity formalism. Therefore, we now go through some of the basic ideas and principles of the spinor-helicity method¹⁶.

3.2.1 Massless Particles

Before describing the spinor-helicity formalism for massless particles, it is worth discussing briefly what we mean by a massless particle. If the magnitude of the three-momentum $|\vec{p}|$ of a particle is much larger than its mass m , the energy of that particle is approximately equal to its three-momentum

$$E = \sqrt{m^2 + |\vec{p}|^2} = |\vec{p}| \sqrt{1 + \frac{m^2}{|\vec{p}|^2}} \approx |\vec{p}| \left(1 + \frac{m^2}{2|\vec{p}|^2} \right) \approx |\vec{p}|, \quad (3.8)$$

and therefore the particle is approximately massless. In the context of this thesis, we are interested in calculations of hard particles which typically have a three-momentum above

¹⁶Note that since paper I includes a fully self-contained introduction to the spinor-helicity formalism, we only introduce the underlying concepts and a small subset of the mathematical tricks here.

about 20 GeV. In this case, all Standard Model particles except for the top quark, H , Z and W^\pm bosons are approximately massless. (The heaviest particle outside of these is the b quark, which has a mass of about 4 GeV. Therefore, a 20 GeV b quark has energy $E \approx 20(1 + 0.02) \approx 20$ GeV according to eq. (6.8), so the approximation is valid for most purposes.)

The spinor-helicity formalism is particularly useful for calculating Feynman diagrams involving massless particles, especially massless spinors.¹⁷ The main reason is that for massless spinors, the chirality projection operator $P_{R/L}$ (see eq. (2.26)) projects out not only a representation of the Lorentz group, but also a helicity state:

$$\begin{aligned} u^+(p) &= v^-(p) = \begin{pmatrix} 0 \\ |p\rangle \end{pmatrix}, & u^-(p) &= v^+(p) = \begin{pmatrix} |p\rangle \\ 0 \end{pmatrix}, \\ \bar{u}^+(p) &= \bar{v}^-(p) = (\langle p| \ 0), & \bar{u}^-(p) &= \bar{v}^+(p) = (0 \ \langle p|), \end{aligned} \quad (3.9)$$

where we use, and will now expand upon, the bras and kets first introduced in eq. (2.27). If we contract a square (angle) bra with a square (angle) ket, we obtain a spinor inner product

$$\langle ij \rangle = -\langle ji \rangle \equiv \langle i||j \rangle, \quad [ij] = -[ji] \equiv [i||j], \quad (3.10)$$

where we use the shorthand $i \equiv p_i$, and note that the inner product is antisymmetric in its arguments, implying that

$$\langle ii \rangle = [jj] = 0. \quad (3.11)$$

These inner products are well-known complex numbers, being different complex square roots of the momentum invariant $s_{ij} = (p_i + p_j)^2 = 2p_i \cdot p_j$:

$$\langle ij \rangle = [ji]^* = e^{i\phi_{ij}} \sqrt{s_{ij}}, \quad \langle ij \rangle [ji] = s_{ij}, \quad (3.12)$$

for some phase $e^{i\phi_{ij}}$ which can be calculated from the explicit representations of the two-component spinors given in papers I and II.

Except for in paper V and the beginning of paper IV, for the remainder of this thesis we repurpose the Feynman slash notation to mean a vector contracted with a Pauli matrix, and any such massless slashed momentum can be rewritten as an outer product of spinors

$$\not{p} \equiv p^\mu \sigma_\mu \stackrel{p^2=0}{=} |p\rangle \langle p|, \quad \bar{\not{p}} \equiv p^\mu \bar{\sigma}_\mu \stackrel{p^2=0}{=} \langle p| [p], \quad (3.13)$$

¹⁷It should be noted that one of the big successes of the spinor-helicity formalism is that it can be used to skip Feynman diagrams entirely, and instead obtain occasionally remarkably simple formulae like the Parke-Taylor formula [41] for the full amplitude. However, this is outside the scope of this thesis, and the interested reader should instead see e.g. [11, 12, 42].

allowing an easy way to show that the spinors in eq. (3.9) solve the massless Dirac equation (also known as the Weyl equation), e.g.

$$p_\mu \gamma^\mu u^+(p) = \not{p}|p\rangle = |p\rangle \underbrace{\langle p|p\rangle}_{\equiv \langle pp\rangle} = 0, \quad p_\mu \gamma^\mu u^-(p) = \bar{\not{p}}|p\rangle = |p\rangle \underbrace{\langle p|p\rangle}_{\equiv [pp]} = 0, \quad (3.14)$$

where we used eq. (3.11).

In Feynman diagrams, it is common to find combinations like $\bar{u}^h(i)\gamma^\mu v^h(j)$, manifesting as

$$\langle i|\bar{\sigma}^\mu|j\rangle \equiv \sqrt{2}\langle i|\bar{\tau}^\mu|j\rangle, \quad \text{or} \quad [i|\sigma^\mu|j\rangle \equiv \sqrt{2}[i|\tau^\mu|j\rangle, \quad (3.15)$$

where we introduce the differently-normalised Pauli matrices $\tau^\mu = \sigma^\mu/\sqrt{2}$ and $\bar{\tau}^\mu = \bar{\sigma}^\mu/\sqrt{2}$. To remove these Pauli matrices and obtain just spinors and spinor-inner products, we use the Fierz identities

$$\langle i|\bar{\tau}^\mu|j\rangle[k|\tau_\mu|l\rangle = \langle i|\bar{\tau}^\mu|j\rangle\langle l|\bar{\tau}_\mu|k\rangle = \langle il\rangle[kj], \quad (3.16)$$

where we used charge conjugation of a spinor line

$$\begin{aligned} \langle i|\bar{\tau}^{\mu_1} \dots \bar{\tau}^{\mu_{2n+1}}|j\rangle &= [j|\tau^{\mu_{2n+1}} \dots \tau^{\mu_1}|i\rangle, \\ \langle i|\bar{\tau}^{\mu_1} \dots \tau^{\mu_{2n}}|j\rangle &= -\langle j|\bar{\tau}^{\mu_{2n}} \dots \tau^{\mu_1}|i\rangle, \\ [i|\tau^{\mu_1} \dots \bar{\tau}^{\mu_{2n}}|j\rangle &= -[j|\tau^{\mu_{2n}} \dots \bar{\tau}^{\mu_1}|i\rangle, \end{aligned} \quad (3.17)$$

where every τ is followed by a $\bar{\tau}$ and vice versa.

Polarisation vectors can also be described in terms of Weyl spinors and a Pauli matrix. We describe an incoming polarisation vector of momentum p and helicity $h = \pm$ using

$$\epsilon_+^\mu(p, r) = \frac{\langle p|\bar{\tau}^\mu|r\rangle}{[pr]} = \frac{[r|\bar{\tau}^\mu|p\rangle}{[pr]}, \quad \epsilon_-^\mu(p, r) = \frac{\langle r|\bar{\tau}^\mu|p\rangle}{\langle rp\rangle} = \frac{[p|\bar{\tau}^\mu|r\rangle}{\langle rp\rangle}, \quad (3.18)$$

where the outgoing polarisation vectors $(\epsilon_\pm^\mu)^*$ are the same as the incoming ones with the opposite polarisation, i.e. $(\epsilon_\pm^\mu)^* = \epsilon_\mp^\mu$, and r is an arbitrary reference vector which corresponds to a gauge choice,¹⁸ and satisfies $r^2 \neq 0$ and $r \cdot p \neq 0$. We can show that these polarisation vectors satisfy the usual normalisation condition from eq. (2.30), namely $\epsilon_h(p) \cdot (\epsilon_{h'}(p))^* = -\delta_{hh'}$, by using the Fierz identity, eq. (3.16),

$$\begin{aligned} \epsilon_+(p, r) \cdot (\epsilon_+(p, r))^* &= \epsilon_+(p, r) \cdot \epsilon_-(p, r) = \frac{\langle p|\bar{\tau}^\mu|r\rangle}{[pr]} \frac{\langle r|\bar{\tau}_\mu|p\rangle}{\langle rp\rangle} = \frac{\langle pr\rangle}{[pr]\langle rp\rangle} = -1, \\ \epsilon_+(p, r) \cdot (\epsilon_-(p, r))^* &= \epsilon_+(p, r) \cdot \epsilon_+(p, r) = \frac{\langle p|\bar{\tau}^\mu|r\rangle}{[pr]} \frac{\langle p|\bar{\tau}_\mu|r\rangle}{[pr]} = \frac{\langle pp\rangle}{[pr][pr]} = 0, \\ \text{etc. ,} \end{aligned} \quad (3.19)$$

¹⁸Changing $r \rightarrow r'$ changes $\epsilon^\mu \rightarrow \epsilon^\mu + \alpha p^\mu$ for some constant α , i.e. changing r we gain a term proportional to the momentum of the polarisation vector, so this is indeed a gauge choice.

while their orthogonality to their momentum follows from the Weyl equation, eq. (3.14),

$$p \cdot \epsilon_+(p, r) = \frac{[r|\not{p}|p]}{[pr]} = 0, \quad p \cdot \epsilon_-(p, r) = \frac{\langle r|\not{p}|p]}{[pr]} = 0, \quad (3.20)$$

Since r corresponds to a gauge choice, any gauge-invariant quantity is r -independent, allowing an easy consistency check of a calculation. Further, while there is no ‘correct’ choice of r , the most useful choice is to set $r_i = p_j$ for particle j being a particle with opposite chirality¹⁹ to particle i . This ensures that inner products like $\langle r_i p_j \rangle = \langle p_j p_j \rangle = 0$ as in eq. (3.11), often allowing to significantly reduce the number of Feynman diagrams under consideration.

We now return to the example from the previous section, and show how the spinor-helicity formalism simplifies the calculation. According to the Feynman rules, the fermion-photon vertex contains either a τ or a $\bar{\tau}$, each of which changes a **left**-chiral fermion into a **right**-chiral one or vice versa. Therefore, the only helicity configurations we need are those where both the electron and positron, and the muon and antimuon, have pairwise opposite chiralities. Further, QED obeys CP symmetry, so the squared matrix element for one set of helicities is the same as the squared matrix element when every particle has swapped its helicity. Therefore, we need to calculate

$$\left| \begin{array}{c} e^-(2) \\ \swarrow \quad \searrow \\ \text{---} \text{wavy line} \text{---} \\ \swarrow \quad \searrow \\ e^+(1) \quad \mu^-(4) \end{array} \right|^2 = 2 \left| \begin{array}{c} e_R^-(2) \\ \swarrow \quad \searrow \\ \text{---} \text{wavy line} \text{---} \\ \swarrow \quad \searrow \\ e_L^+(1) \quad \mu_R^-(4) \end{array} \right|^2 + 2 \left| \begin{array}{c} e_R^-(2) \\ \swarrow \quad \searrow \\ \text{---} \text{wavy line} \text{---} \\ \swarrow \quad \searrow \\ e_L^+(1) \quad \mu_L^-(4) \end{array} \right|^2, \quad (3.21)$$

where the Feynman diagrams on the right have explicit chiralities (equivalent to explicit helicities for massless particles) and are called helicity diagrams.

To calculate each helicity diagram, we use eq. (3.9) for the external spinors, the vertex is (up to couplings) given by the Dirac matrix γ^μ , which we write in the chiral basis as in eq. (2.23), we again use the Feynman gauge (see section 2.4), and use the Fierz identity,

¹⁹We define the chirality of a gauge boson as the chirality of the spinor containing its momentum p in eq. (3.18). For example, if $\epsilon^\mu(p, r) \sim \langle p|\bar{\tau}^\mu|r]$, then we think of the photon as having **right** chirality since $\langle p|$ is a **right**-chiral spinor.

eq. (3.16) to obtain inner products

$$\begin{aligned}
 \begin{array}{c} e_R^-(2) \\ e_L^+(1) \end{array} \rightarrow \begin{array}{c} \mu_L^+(3) \\ \mu_R^-(4) \end{array} &= \frac{-2i^3 e^2}{s_{12}} [1|\tau^\mu|2\rangle\langle 4|\bar{\tau}_\mu|3] = \frac{2ie^2}{s_{12}} [13]\langle 42\rangle, \\
 \begin{array}{c} e_R^-(2) \\ e_L^+(1) \end{array} \rightarrow \begin{array}{c} \mu_R^+(3) \\ \mu_L^-(4) \end{array} &= \frac{-2i^3 e^2}{s_{12}} [1|\tau^\mu|2\rangle[4|\tau_\mu|3] = \frac{2ie^2}{s_{12}} [14]\langle 32\rangle.
 \end{aligned} \tag{3.22}$$

Notice that, as predicted at the end of section 3.1, the amplitude is now written as square roots of the momentum invariants s_{ij} (recall from eq. (3.12) that $\sqrt{s_{ij}} \sim \langle ij \rangle \sim [ij]$).

Starting at eq. (3.22), we see that the inner products are between spinors with the same chiralities, as if the spin structure gave momentum flowing from one chiral spinor to another of the same type. This extends the final comment of section 3.1, and will be transparent in the chirality-flow formalism.

To finish the calculation, we use eq. (3.12) to square the amplitudes, obtaining

$$\begin{aligned}
 \left| \begin{array}{c} e^-(2) \\ e^+(1) \end{array} \rightarrow \begin{array}{c} \mu^+(3) \\ \mu^-(4) \end{array} \right|^2 &= 2 \left| \begin{array}{c} e_R^-(2) \\ e_L^+(1) \end{array} \rightarrow \begin{array}{c} \mu_L^+(3) \\ \mu_R^-(4) \end{array} \right|^2 + 2 \left| \begin{array}{c} e_R^-(2) \\ e_L^+(1) \end{array} \rightarrow \begin{array}{c} \mu_R^+(3) \\ \mu_L^-(4) \end{array} \right|^2 \\
 &= 2 \left[\frac{4e^4}{s_{12}^2} s_{13}s_{24} + \frac{4e^4}{s_{12}^2} s_{14}s_{23} \right] \\
 &= \frac{8e^4}{s_{12}^2} [s_{13}s_{24} + s_{14}s_{23}],
 \end{aligned} \tag{3.23}$$

as before, in eq. (3.7). This new calculation was much quicker and easier than before. Crucially, the amplitude was a complex number rather than a matrix, meaning that computer simulations using this method are much quicker than those using the method of section 3.1.

3.2.2 Massive Particles

The spinor-helicity formalism can also be easily used for massive particles, but, particularly for massive fermions, it loses some of its useful properties such as the correlation between helicity and chirality. Nonetheless, it maintains the property that amplitudes are now a complex number rather than a matrix, meaning that it is copiously used in computer calculations.

There are two common approaches to the spinor-helicity formalism for massive particles, The one we used in papers II and IV²⁰ is to choose an arbitrary direction vector q satisfying $(q)^2 = 0$, which defines (but is not equal to) the spin axis s , and defines a split of the massive momentum p into two massless momenta [39, 44, 45]

$$p = p^\flat + \frac{p^2}{2p^\flat \cdot q} q, \quad s = \frac{1}{m} \left(p^\flat - \frac{p^2}{2p^\flat \cdot q} q \right), \quad (3.24)$$

allowing to recycle results from massless spinor helicity such as

$$\not{p} = \not{p}^\flat + \frac{p^2}{2p^\flat \cdot q} \not{q} = |p^\flat\rangle\langle p^\flat| + \frac{p^2}{2p^\flat \cdot q} |q\rangle\langle q|. \quad (3.25)$$

Spinors now have both their **left**- and **right**-chiral parts, with for example

$$u^+(p) = \begin{pmatrix} \frac{m}{[p^\flat q]} |q\rangle \\ |p^\flat\rangle \end{pmatrix}, \quad v^-(p) = \begin{pmatrix} -\frac{m}{[p^\flat q]} |q\rangle \\ |p^\flat\rangle \end{pmatrix}, \quad (3.26)$$

which smoothly go to their massless limits by taking $m \rightarrow 0$ and $p^\flat \rightarrow p$. The full set of spinors is not central to the discussion and is given in paper II, so is not repeated here.

As described in section 2.1.1, a massive vector boson has three spin degrees of freedom, whereas a massless one has two. While at first this appears to need a strong overhaul to the polarisation vectors, the transverse polarisation vectors are instead left unchanged compared to massless ones in eq. (3.18), except for replacing $r \rightarrow q$ and $p \rightarrow p^\flat$, while the third polarisation vector is equal to the spin direction vector, $\epsilon_0^\mu(p, q) = s^\mu$.

With these prescriptions, we have rewritten all massive objects as combinations of massless spinors, allowing to recycle the massless spinor-helicity formalism. However, we have a more clunky formalism, and, in contrast to the gauge reference momentum r , the reference vector q is physical since it defines the spin direction s . Therefore, a spin-amplitude, i.e. the amplitude for a given set of spins, is dependent on q , and only after summing over all spins does the dependence on q disappear (compare this to the helicity-amplitude being independent of the gauge reference choice r).

3.3 Berends-Giele Recursions

In the above sections we have calculated scattering amplitudes using Feynman diagrams. This is a process which always works and is useful, but which has its flaws. One of the main

²⁰The alternative approach is that proposed in [43], however this approach is not used in this thesis so will not be discussed here.

flaws of Feynman diagrams is that their multiplicity grows like a (double) factorial with the number of external particles [46]. Therefore, calculating scattering amplitudes without Feynman diagrams can be very advantageous, and there is a whole community finding new and exciting ways to do so (see e.g. [11, 12] for an overview of such methods).

The oldest, and often fastest [21–23], way to calculate amplitudes without Feynman diagrams, is off-shell Berends-Giele (BG) recursion [20]. BG recursion works by building up off-shell n -particle currents by summing together smaller off-shell currents. This can be done for any amplitude, involving any number of spinors and bosons, and is most useful for QCD amplitudes since the number of Feynman diagrams is particularly high and reducing this is important. For this reason, in paper V, we revived an old branch of the MadGraph5_aMC@NLO event generator (see section 5) which, among other things, aimed to use these recursions to speed up the amplitude calculation.

The formulae and an explanation of the different BG currents are given in paper V, so we will not go through them here in detail. Instead, we show the all-gluon recursion to give an example of how this is different to a Feynman diagram calculation and why it can improve calculation speeds. The base ingredients of the all-gluon recursion are a polarisation vector, which acts as the one-particle current J_1^μ , and a three-gluon vertex with one particle off-shell, which acts as the two-particle current J_2^μ :

$$\begin{aligned} J_1^\mu(1) &= \epsilon^\mu(1) , \\ J_2^\mu(1, 2) &= \frac{-i}{(p_1 + p_2)^2} V_3^{\mu\mu_1\mu_2}(p_1, p_2) J_{1,\mu_1}(1) J_{1,\mu_2}(2) , \end{aligned} \quad (3.27)$$

where $\epsilon^\mu(1)$ is the gluon polarisation vector with momentum p_1 , and $V_3^{\mu\mu_1\mu_2}(p_1, p_2)$ the three-gluon vertex, see papers I and II for its form. An n -gluon current is then given by

$$\begin{aligned} J_n^\mu(1, \dots, n) &= \frac{-i}{P_{1,n}^2} \times \\ &\left\{ \sum_{i=1}^{n-1} V_3^{\mu\nu\rho}(P_{1,i}, P_{i+1,n}) J_\nu(1, \dots, i) J_\rho(i+1, \dots, n) + \right. \\ &\left. \sum_{i=1}^{n-2} \sum_{j=i+1}^{n-1} V_4^{\mu\nu\rho\sigma} J_\nu(1, \dots, i) J_\rho(i+1, \dots, j) J_\sigma(j+1, \dots, n) \right\}, \end{aligned} \quad (3.28)$$

where $V_4^{\mu_1\mu_2\mu_3\mu_4}$ is the four-gluon vertex (see papers I and II), we use the shorthand $P_{1,n}^2 = (p_1 + \dots + p_n)^2$, and we drop the number of particles n in J_n^μ where convenient. To turn an n -point current into an $(n+1)$ -particle amplitude, we need to amputate the off-shell propagator and multiply by the remaining polarisation vector

$$M(1, \dots, n+1) = \epsilon_\mu(n+1) \frac{p_{1,n}^2}{-i} J_n^\mu(1, \dots, n) . \quad (3.29)$$

Note that, while we use the Feynman rules for the vertices, particles, and propagators in eqs. (3.27) and (3.28), we build the amplitude very differently. Instead of calculating individual Feynman diagrams, at each point of the recursion we sum together multiple partial Feynman diagrams into a single off-shell current, and then at the end we turn this into an amplitude using eq. (3.29). Therefore, using eqs. (3.27) - (3.29) to calculate the amplitude can lead to a decrease in the number of terms required compared to Feynman diagram calculations.²¹ It also allows to prove some analytical formulae such as the Parke-Taylor formula for MHV amplitudes [20, 41].

4 QCD and Colour

In Paper V we describe a new algorithm to calculate colour in `MadGraph5_aMC@NLO` (MG5aMC), and also use that algorithm to simplify colour calculations by using an expansion in the number of colours N_c [47]. Additionally, the chirality-flow formalism of papers I-IV was inspired by the idea of colour flow [48], which uses flow lines instead of index algebra to do calculations more transparently and quickly in colour space. Therefore, in this section we briefly describe what the colour algebra is, why we need it, how to do colour calculations, what an expansion in the number of colours is and why it could be useful, and what colour flow is and how it is linked to chirality flow.

QCD is a gauge theory obeying the non-abelian symmetry group $SU(N_c)$ with $N_c = 3$. Unlike QED, which obeys the abelian $U(1)$ symmetry group, the generators of QCD are matrices. Therefore, in the Feynman rules of QCD (see papers I and II), vertices do not just contain the coupling g_s multiplied by a constant charge factor, but contain the coupling multiplied by a generator of the gauge group: either the fundamental generator t_{ij}^a if the interaction is between a quark and a gluon, or the adjoint generator f^{abc} if the gluons are interacting with themselves.²²

This implies that any QCD amplitude is a function of the QCD generators of each particle involved, the momenta of each particle, and their helicities or spins. A common trick is to factorise the colour part of an amplitude from the kinematics [48–51]

$$\mathcal{M}(\text{su}(N_c); p_1, h_1; \dots, p_n, h_n) = \sum_{\sigma} F_{\sigma}(\text{su}(N_c)) M_{\sigma}(p_1, h_1; \dots; p_n, h_n), \quad (4.1)$$

²¹Note that our implementation of BG currents in paper V was actually less efficient and therefore slower than the standard implementation of Feynman diagrams in `MadGraph5_aMC@NLO`, but this was because we did not properly optimise the code. Other codes have found BG recursion to be the fastest possible method available [21–23].

²²Here $i, j = 1, 2, \dots, N_c$ are fundamental colour indices, and $a, b, c = 1, 2, \dots, N_c^2 - 1$ are adjoint colour indices.

where σ runs over all basis vectors of the chosen basis in $\text{su}(N_c)$, F_σ is a function of the gauge algebra $\text{su}(N_c)$, and M_σ is the kinematic (colour-ordered) amplitude, which is a function of the momenta and helicities or spins of the particles, and is usually calculated using the tools described in section 3. Depending on the basis in colour space, there may be different forms of F_σ and M_σ .

The squared matrix-element is then given by,

$$|\mathcal{M}(1, \dots, n)|^2 = \sum_{\sigma, \sigma'} M_\sigma \underbrace{F_\sigma F_{\sigma'}^*}_{C_{\sigma\sigma'}} M_{\sigma'}^*, \quad (4.2)$$

where we have dropped all functional dependence on the right hand side; σ, σ' are two sets of colour-orderings; and the product $F_\sigma F_{\sigma'}^* \equiv C_{\sigma\sigma'}$ is often called the colour matrix, and can be calculated using the following colour-algebra relations:

$$\begin{aligned} \text{Tr}(t^a) &= 0, & \text{Tr}(t^a t^b) &= T_R \delta^{ab}, \\ i f^{abc} &= \frac{1}{T_R} \text{Tr}(t^a [t^b, t^c]), & i f^{abc} t^c &= [t^a, t^b], \\ \delta_{ii} &= N_c, & \delta^{aa} &= N_c^2 - 1, \\ t_{ij}^a t_{kl}^a &= T_R \left(\delta_{il} \delta_{jk} - \frac{1}{N_c} \delta_{ij} \delta_{kl} \right), \end{aligned} \quad (4.3)$$

where T_R is a normalisation factor. Since in eq. (4.2) we square the colour terms, the colour matrix contains traces of the generators, and therefore each term of that matrix is a polynomial in the number of colours N_c . Expanding this matrix in powers N_c is one of the main topics of paper V, and will be discussed next.

4.1 Expansion in the Number of Colours

The MG5aMC event generator described in section 3 uses the fundamental basis to calculate eq. (4.1). In this basis, the colour matrix $C_{\sigma\sigma'}$ in eq. (4.2) is (depending on the process) roughly an $n! \times n!$ matrix for $n \sim$ the number of gluons. As the particle multiplicity increases, the colour matrix quickly becomes the bottleneck in any QCD calculation [52]. Since the current versions of our event generators are incompatible with the proposed computer budget of CERN and its experiments [53, 54], alleviating this bottleneck is important work.

There are several possible solutions to this problem. One possible solution is to change the colour basis to a diagonal basis such as the multiplet basis [55–58]. Using this solution is arguably the most pleasing, since it removes a dimension from the colour matrix, thus making it much quicker to use while also keeping the full accuracy of the scattering amplitude.

Another possible solution is an approximate one, and is the option taken in paper V. In this solution, we reduce the number of terms in the colour matrix by expanding it in the number of colours N_c , and only keep terms with a high-enough power of N_c [47]. This approximation is effective because each term in the colour matrix $C_{\sigma\sigma'}$ has the form²³

$$C_{\sigma\sigma'} = a_n N_c^n + a_{n-2} N_c^{n-2} + a_{n-4} N_c^{n-4} + \dots, \quad (4.4)$$

where a_n, a_{n-2}, \dots are constants, and only some terms, called the leading colour (LC) terms, have $a_n \neq 0$, some other terms called next-to-leading colour (NLC) have $a_n = 0$ and $a_{n-2} \neq 0$, next-to-next-to-leading colour (N2LC) terms have $a_n = a_{n-2} = 0$ and $a_{n-4} \neq 0$, etc. Therefore, this colour expansion is actually an expansion in N_c^2 , with each term about $1/N_c^2 \approx 0.11$ the size of the previous term. Therefore, the colour expansion is naively about as accurate as the expansion in the strong coupling $\alpha_s(M_Z) \approx 0.12$ [17].

In the fundamental basis used in paper V, a given colour matrix will typically have the LC terms on the diagonal, the NLC terms on the diagonal and/or off-diagonal, and N2LC or higher terms all on the off-diagonal. Keeping only some terms of the expansion is then equivalent to turning the full $n! \times n!$ colour matrix into a sparse matrix, which can be summed over much quicker. Further, it was shown in [59] that at NLC accuracy, only a small subset of the rows of the colour matrix is needed when integrating the matrix element over phase-space, and therefore we can calculate matrix elements far quicker and for a higher particle multiplicity than if we calculate them at full colour.

Of course this is just an approximation, and a key question to this approximation is how accurate and precise, and therefore how reliable it is in practice? We were able to answer these questions in paper V for tree-level QCD processes with at most 8 particles.

4.2 Colour Flow

As described in section 4, to go from some basis to the colour matrix we need to use the relations in eq. (4.3) over and over until we obtain a polynomial in N_c . While doing this algebraically with index algebra works, a more conceptual and error-free method was created [47, 60–62], which was eventually called colour flow [48]. In this method, we first use crossing symmetry, which allows us to calculate the scattering amplitude for a $0 \rightarrow n+2$ process instead of a $2 \rightarrow n$ one. This has the advantage that we have the same number of quarks and antiquarks, and that all particles are on the same footing so permuting them is simple. Next, we draw quark lines to represent a fundamental colour index, antiquark lines to represent a fundamental anticolour index, and draw gluon lines to represent an adjoint index.

²³Strictly speaking this form of the colour matrix only holds if there are no identical quark lines, in which case each term is only one power of N_c smaller than the previous one (see paper V).

$$if^{abc} = \text{diagram} = \text{diagram} - \text{diagram} = \text{Tr}(t^a[t^b, t^c])$$

$$\text{diagram} = \text{diagram} - \frac{1}{N} \text{diagram}$$

Figure 5: Two examples of equations from eq. (4.3) written using colour flow. Note that we set the normalisation $T_R \rightarrow 1$.

In a given colour calculation (see figure 5 for examples) we adhere to the following process:

- Draw the colour lines as just described
- Replace structure functions f^{abc} using $if^{abc} = \frac{1}{T_R} \text{Tr}(t^a[t^b, t^c])$ until we only have quark lines with gluon lines joining them
- Use the Fierz identity, $t_{ij}^a t_{kl}^a = T_R \left(\delta_{il} \delta_{jk} - \frac{1}{N_c} \delta_{ij} \delta_{kl} \right)$ to remove all adjoint indices
- When squaring, each closed loop is a factor of N_c .

We now have a conceptually simple way to calculate colour factors belonging to a given (squared) diagram or amplitude. Indeed, we can make this quicker by associating a double line to each gluon, a single line to each (anti)quark, and joining them in all possible ways without going through the formal procedure outlined above.²⁴ This procedure can be done for any $\text{su}(N_c)$ algebra. In section 2.1, we explained that the Lorentz algebra could be recast as two copies of $\text{su}(2)$, so we expect that also the kinematic amplitude which comes from this Lorentz algebra can be calculated using an analogue of this colour flow. Indeed, that is precisely the main idea of this thesis, underpinning the chirality-flow formalism of papers I-IV.

5 Automating Scattering Amplitudes using MadGraph5_aMC@NLO

Up until now we have described and shown some examples of how to calculate a scattering amplitude analytically. In theory, we can take this analytical squared matrix element and

²⁴One has to be careful with minus signs when using this shortcut.

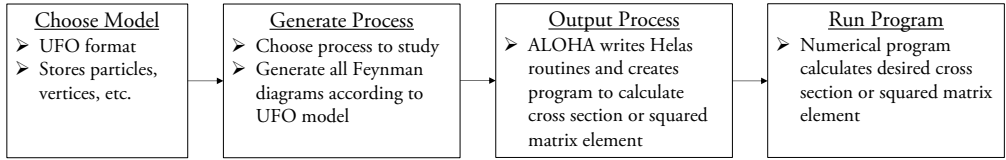


Figure 6: The workflow of the MG5aMC event generator.

analytically integrate over it according to eq. (3.1). In practice however, this is not possible. Instead, we both calculate the matrix element and do the integral numerically, which requires evaluating the (squared) scattering amplitude at possibly millions of different phase-space points. This is clearly not something which can be done with a pen and paper, so we use computer programs instead, with some of the most common programs for tree-level calculations being AlpGen [63], Comix [64], HELAC [65], MadGraph5_aMC@NLO [66], O'Mega [67], and WHIZARD [68].

In this thesis, we use the MadGraph5_aMC@NLO program (MG5aMC) to calculate scattering amplitudes in massless QED using the chirality-flow formalism in paper III, and use it in paper V to calculate QCD amplitudes with BG recursions and an expansion in the number of colours. Therefore, we dedicate this section to describing the MG5aMC event generator itself, what it can do, and how it does it.

MG5aMC is a metacode which creates HELAS routines [69] in Fortran²³ to calculate either the squared matrix element (standalone mode) or the cross section (using MadEvent) for a given process within a given model. The user has full control over the model, which is written in the UFO format [70]. MG5aMC works out all possible Feynman diagrams according to the model, and then uses ALOHA [71] to write the output HELAS routine. The user then runs the output HELAS program to get their desired result. This workflow is summarised in figure 6.

We will now go through each step in some detail, stressing those points relevant for papers III and V.

5.1 HELAS

MG5aMC uses the HELAS method to numerically calculate matrix elements. The name HELAS is an acronym for Helicity Amplitude Subroutines [69], and is a play on the Japanese word *helású*, which means to decrease, chosen because the program uses caching and recycling to decrease the amount of work required to calculate a helicity amplitude.

²³HELAS routines in C++ and Python can also be created.

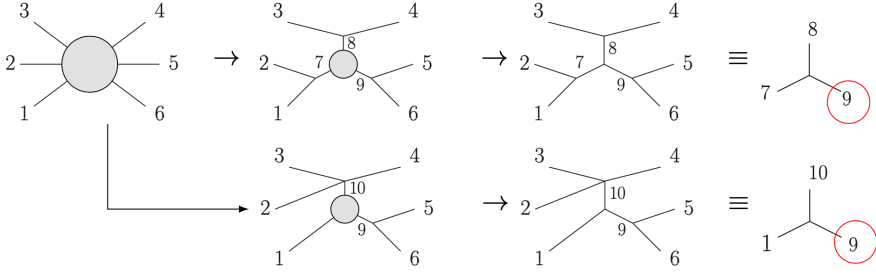


Figure 7: An example of recycling in the HELAS method. All particles, both internal and external, are drawn as straight lines and given a number to label them. The blob implies a not-yet-calculated interaction. Particle 9 is common to both Feynman diagrams and is only calculated once, cached, and recycled for the second diagram. At each point in the calculation HELAS will calculate a local three-point interaction involving either on-shell (external) or off-shell (internal) particles. Figure taken from figure 1 in paper V.

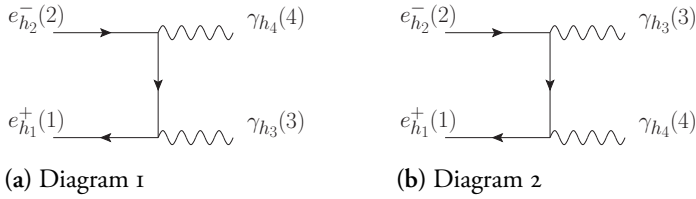


Figure 8: The two Feynman diagrams in $e_{h_1}^+(1)e_{h_2}^-(2) \rightarrow \gamma_{h_3}(3)\gamma_{h_4}(4)$

The two main realisations which have made HELAS a success are that helicity amplitudes allow to square complex numbers, which, as stated in section 3, is faster than squaring a matrix and then taking its trace; and that external and internal particles such as propagators are common to multiple Feynman diagrams in a given process. HELAS takes these common propagators and calculates them only once, caches them, and then uses their result in subsequent diagrams (see figure 7). This trick is called recycling and is key to the fast evaluation speed of HELAS.

Perhaps the simplest way to explain how HELAS works is through an example. Imagine we want to calculate the matrix element for $e_{h_1}^+(1)e_{h_2}^-(2) \rightarrow \gamma_{h_3}(3)\gamma_{h_4}(4)$. We have to

choose a given helicity configuration h_1, \dots, h_4 and calculate the amplitude

$$\begin{aligned}
M(e_{h_1}^+(1)e_{h_2}^-(2) \rightarrow \gamma_{h_3}(3)\gamma_{h_4}(4)) = \\
\underbrace{\bar{v}_{h_1}(1)ie\gamma_\mu\epsilon_{h_3}^\mu(3)\frac{i(p_2-p_4)_\rho\gamma^\rho}{s_{24}}ie\gamma_\nu u_{h_2}(2)\epsilon_{h_4}^\nu(4)}_{\psi(5)} \\
+ \underbrace{\bar{v}_{h_1}(1)ie\gamma_\mu\epsilon_{h_4}^\mu(4)\frac{i(p_2-p_3)_\rho\gamma^\rho}{s_{23}}ie\gamma_\nu u_{h_2}(2)\epsilon_{h_3}^\nu(3)}_{\psi(6)}, \quad (5.1)
\end{aligned}$$

where the first line is the Feynman diagram in figure 8a, and the second line is the Feynman diagram in figure 8b.

HELAS does the calculation in eq. (5.1) by first calculating all external wavefunctions once only (we can recycle the results for the wavefunction in each diagram), then combining particle 1 with the vertex factor $ie\gamma_\mu$, particle 3, and the propagator in the first diagram, calling the resultant off-shell particle $\psi(5)$; next combining particles 1 and 4 with their vertex and multiplying by the second diagram's propagator, calling the resultant off-shell particle $\psi(6)$; then combining particle 5 with particles 2 and 4 to get diagram one, and combining particle 6 with particles 2 and 3 to get diagram two.

The key here is that each n -point vertex is calculated separately. Either, $n - 1$ particles are multiplied by the coupling and the propagator to create a new off-shell particle, or, all n particles are multiplied by the coupling to create the complex number for this Feynman diagram. All Dirac matrices and on-shell wavefunctions are given an explicit representation, and the matrix multiplication is done using brute force. At no point do we do any analytic simplifications in the same spirit as in section 3.2, since it is considered more efficient to do the matrix multiplication than the analytic simplification which removes γ -matrices and obtains spinor-inner products.

One of the big achievements of this thesis is that we have developed chirality flow, which makes the analytic simplifications almost trivial. Therefore, it should be possible to improve the speed of the HELAS routine by removing most of the matrix multiplication. In paper III, we showed that this is indeed true, at least for massless QED calculations, finding an increase in evaluation speed of up to a factor of 10. At the time of writing this thesis, I am helping two Master students extend the automation of chirality flow in MG5aMC to the rest of the (tree-level) Standard Model.

In paper V of this thesis, we updated the HELAS routine in two different ways. One big update was that it combines off-shell currents into the BG currents of section 3.3, instead of keeping them separate to calculate separate Feynman diagrams. This procedure can be thought of as upgrading the recycling, since many currents are combined into one which

can still be recycled, meaning less work will be done by HELAS.²⁶ The second main update was to the sum over colours

$$|\mathcal{M}(1, \dots, n)|^2 = \sum_{\sigma, \sigma'} M_{\sigma} \underbrace{F_{\sigma} F_{\sigma'}^*}_{C_{\sigma\sigma'}} M_{\sigma'}^*, \quad (5.2)$$

where we repeated eq. (4.2) here for convenience. It is not shown in the example above, but in MG5aMC and HELAS the colour matrix $C_{\sigma\sigma'}$ is printed in its entirety before calculating the wavefunctions and whole Feynman diagrams. Then, the Feynman diagrams are summed together into their kinematic amplitudes M_{σ} , and the double sum of eq. (5.2) is done as two Fortran do loops. In paper V, we no longer give a full colour matrix, but only one row, and update the colour sum so that it is simple to only include those terms at LC, NLC, etc. Doing this was the main optimisation in paper V and helped reduce the bottleneck of colour in QCD calculations, even at full colour.

5.2 UFO Models and Diagram Generation

In order to write chirality flow into MG5aMC, we had to create a Universal FeynRules Output (UFO) model with chiral particles and chiral interactions. In this section we describe the UFO format and our model in a bit of detail, as this information is skipped over in paper III.

A UFO model is an abstract Python module which contains all of the information which is required to calculate a matrix element in this model [70]. The information needed to specify the (leading order) UFO model is

- A set of particles and their quantum numbers (spin, charges, etc.)
- A set of parameters (e.g. masses, coupling constants, etc.)
- A set of vertices describing the interactions between different particles (coming from a given Lagrangian).

The abstract module is not tied to any particular event generator, but was designed in conjunction with MG5aMC as an easy way to generate events in any desired beyond-Standard Model (BSM) study that the user desires. The user usually provides their BSM Lagrangian to a tool like FeynRules [72, 73], which outputs the UFO files; however, as in paper III, we can also write the UFO model directly.

²⁶It should be noted though that our implementation of BG recursion in paper V was sub-optimal and worse than the native HELAS implementation of MG5aMC. Ways to optimise this are known, but the actual optimisation was left to future work.

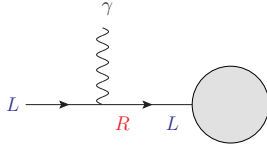


Figure 9: Building Feynman diagrams in chiral massless QED. A **left**-chiral fermion interacts with a photon and becomes a **right**-chiral fermion. However, the off-shell **right**-chiral fermion becomes a **left**-chiral one after propagating to the next vertex (the blob, which represents the rest of the diagram). Therefore, this interaction actually took a **left**-chiral fermion and a photon and created another **left**-chiral fermion, rather than outputting a **right**-chiral one.

Once the user specifies their model and process to generate, MG5aMC tries to create all of the allowed Feynman diagrams. It does this by combining particles sequentially according to the Feynman rules; first combining external particles together into a new list of off-shell internal particles, then combining this new list to create more internal, off-shell, particles, and so on. It repeats this process until it either completes a Feynman diagram by combining all remaining particles together, or until the remaining particles cannot be legally combined, in which case the combination is discarded [66].

In paper III, we created a UFO model with chiral massless QED particles and vertices. Specifically, we created a new set of chiral leptons and photons with the same set of quantum numbers and parameters as in the Standard Model, and created two distinct types of chiral vertices, one with a **left**-chiral fermion, a **right**-chiral antifermion, and a photon; and another with a **right**-chiral fermion, a **left**-chiral antifermion, and a photon. (The Pauli matrix connects **left**- and **right**-chiral particles, as can be seen in eq. (B.15), so e.g. a **left** fermion-**left** anti-fermion-photon vertex is not allowed.) The problem with this setup is that the fermion propagator ($\sim \bar{p} = |p\rangle[p]$ or $\sim p = |p\rangle\langle p|$) changes a **left**-chiral fermion into a **right**-chiral one or vice versa (see eq. (B.13)). In the UFO language, this means that the fermion propagator changes the particle type, something which is not allowed in MG5aMC. Therefore, after combining the particles together in a given vertex, we had to flip the chirality (change particle type) of the off-shell (anti)fermion before going to the next iteration of the sequential combination method (see figure 9).

5.3 ALOHA

After MG5aMC has generated the Feynman diagrams for the process, it uses ALOHA²⁷ to write the HELAS routine which will numerically calculate it (see figure 6). ALOHA is a part of the MG5aMC program which takes a set of Feynman diagrams and the UFO model which

²⁷ALOHA is an acronym for Automatic Libraries of Helicity Amplitudes.

built them as input, and outputs a HELAS routine [71]. This is very useful since it automates the numerical implementation for any possible user-specified model, eliminating the need to spend time writing your own bug-free HELAS routine with consistent conventions.

Unfortunately for us in paper III, we had to update ALOHA and partially write our own sub-routines for HELAS. In particular, ALOHA did not know how to create the simplified Lorentz structures we created in papers I and II, so these had to be put in manually. Additionally, ALOHA was given an input model where each vertex flipped the chirality of the fermion, but a set of vertices where the final particles were often of the same chirality (see figure 9). Therefore, we had to update the UFO model to include these same-chirality vertices before ALOHA created the HELAS routines.

6 Loop Calculations

So far in this thesis, everything has implicitly been at tree-level unless otherwise stated. In this section, we move to the one-loop level, where many complications arise which were not present before. We discuss many of the basic properties of one-loop diagrams, how they are usually calculated, what physics principles have to be reconsidered when including loops in a theory, and link these to paper IV in which we developed chirality flow for one-loop diagrams.

We begin with the fundamental difference between a loop diagram and a tree-level diagram: in one-loop diagrams there is an unconstrained momentum (in this thesis consistently called l) running through the loop, whereas all momenta in tree-level diagrams are constrained. Since this loop momentum is unconstrained, we must integrate over all of its possible values, leading to integrals $I_{i_1 \dots i_k}^4 [N^{\mu_1 \dots \mu_n}]$ of the following form:

$$I_{i_1 \dots i_k}^4 [N^{\mu_1 \dots \mu_n}] \equiv \int_{-\infty}^{\infty} \frac{d^4 l}{(2\pi)^4} \frac{N^{\mu_1 \dots \mu_n}}{D_{i_1} \dots D_{i_k}}, \quad (6.1)$$

where we integrate over the entirety of 4-dimensional energy-momentum space, $N^{\mu_1 \dots \mu_n}$ is some numerator which may be a scalar, vector, or general tensor in Lorentz space, and D_i is a propagator momentum of the form $p^2 - m^2$ where p involves the loop momentum l . The loop momentum l may also appear in the numerator.

6.1 Divergences

The biggest (naive) problem with eq. (6.1), is that it is often infinite. If the infinity occurs when $l \rightarrow 0$, then it is called an infrared, or IR, divergence, and if it occurs when $l \rightarrow \infty$, then it is called an ultraviolet, or UV, divergence. We now briefly discuss how to remove these infinities.



(a) Real correction

(b) Virtual (loop) correction

Figure 10: Two possible sources of IR divergences. Either the emitted particle becomes infinitely soft or collinear to its emitter (a), or the particle in the loop is infinitely soft (b). The KLN theory ensures that these divergences are equal and opposite for IRC-safe observables.

IR Divergences

IR divergences can be either more, or less, tricky to remove, depending on the calculation at hand. In general, removing them is observable dependent. Either the observable is soft and collinear (IRC) unsafe, in which case IR divergences are a problem, or they are IRC safe, in which case the Kinoshita-Lee-Nauenberg (KLN) theorem ensures that all IR divergences of one-loop diagrams are cancelled by an opposite divergence from the emission of an unobservable real particle (see figure 10) [74, 75].

When doing the integral eq. (6.1), what is often done on a practical level is to first assume that the IR divergence is taken care of by adding an IR regulator such as a small mass to all particles, then doing the integral, regulating the UV divergences, and then removing the IR regulator (see e.g. [76]). IR divergences are not important to this thesis, however, so we do not discuss them further.

UV Divergences

UV divergences have to first be regulated in the integral, eq. (6.1), and then removed using renormalisation (see e.g. [10]). Loosely speaking, renormalisation works by recognising that many parameters in the Lagrangian, Feynman rules, and the UV divergences themselves, are unphysical. Therefore, we can remove the UV divergences by redefining some of the other unphysical quantities to have the opposite divergence. After doing this, all physical observable quantities are rendered finite.

Let us take ϕ^4 theory as a simple example of this. The Lagrangian for ϕ^4 theory is equal to eq. (2.18) with only the ϕ^2 and ϕ^4 terms remaining,

$$\mathcal{L} = \frac{1}{2} (\partial_\mu \phi_0) (\partial^\mu \phi_0) - \frac{m_0^2}{2} \phi_0^2 - \frac{\lambda_0}{4!} \phi_0^4, \quad (6.2)$$

where we redefined the unphysical quantities of the Lagrangian with a subscript 0 to be clear that these are unphysical. Such quantities are called the *bare* parameters of the theory.

The physical propagator for a scalar in this theory has the form

$$-\frac{\overset{p}{\longrightarrow}}{\text{phys}} = \frac{iZ}{p^2 - m^2}, \quad (6.3)$$

where m^2 is the physical mass of the particle, and Z an unphysical parameter, which can be eliminated from the physical propagator by a field redefinition

$$\phi_0 = Z^{1/2} \phi, \quad (6.4)$$

giving an updated Lagrangian

$$\mathcal{L} = \frac{Z}{2} (\partial_\mu \phi) (\partial^\mu \phi) - \frac{Z m_0^2}{2} \phi^2 - \frac{Z^2 \lambda_0}{4!} \phi^4, \quad (6.5)$$

for a renormalised field ϕ . Staring at this Lagrangian, we see that $Z^2 \lambda_0$ must contain the physical coupling λ plus some unphysical part, $Z m_0^2$ must contain the physical mass m^2 plus some unphysical part, and that Z must be 1 plus some unphysical part

$$Z = 1 + \delta_Z, \quad Z m_0^2 = m^2 + \delta_m, \quad Z^2 \lambda_0 = \lambda + \delta_\lambda, \quad (6.6)$$

which implies the Lagrangian is

$$\mathcal{L} = \underbrace{\frac{1}{2} (\partial_\mu \phi) (\partial^\mu \phi) - \frac{m^2}{2} \phi^2 - \frac{\lambda}{4!} \phi^4}_{\text{usual Feynman rules}} + \underbrace{\frac{\delta_Z}{2} (\partial_\mu \phi) (\partial^\mu \phi) - \frac{\delta_m}{2} \phi^2 - \frac{\delta_\lambda}{4!} \phi^4}_{\text{counterterms}}, \quad (6.7)$$

where the unphysical pieces give new Feynman rules called counterterms. In renormalisation, we calculate the loop diagrams using the usual Feynman rules, obtain infinities, and then remove these infinities by defining the parameters δ_Z , δ_m , and δ_λ in the counterterms to have equal and opposite divergence. In this way we have renormalised the theory, removed all UV divergences, and can calculate physical quantities without worry.

6.2 Dimensional Regularisation

So far in this section we have described the types of divergences we obtain and an outline of how to remove them. We have not yet, however, given a specific regularisation scheme, i.e., a way to quantify how much the integral diverges. Dimensional regularisation [77–79] is the most commonly used method to quantify these divergences, and is used (though not in the conventional way) in paper IV. Therefore, we briefly describe it here.

Dimensional regularisation works by changing spacetime from 4 dimensions to $d = 4 - 2\epsilon$ dimensions. This implies adding an extra subspace $QS_{[-2\epsilon]}$ to the usual Minkowski space $S_{[4]}$, obtaining

$$QS_{[d]} = S_{[4]} \oplus QS_{[-2\epsilon]}, \quad (6.8)$$

which shows that the extra-dimensional subspace is orthogonal to Minkowski space. Using eq. (6.8), we see that all vectors are split into its 4d and -2ϵ d components, e.g.,

$$g_{[d]}^{\mu\nu} = g_{[4]}^{\mu\nu} + g_{[-2\epsilon]}^{\mu\nu}, \quad \gamma_{[d]}^\mu = \gamma_{[4]}^\mu + \gamma_{[-2\epsilon]}^\mu, \quad (6.9)$$

where we label the dimensionality of an object with a square bracket.

Note that the Lagrangian should be d -dimensional, not 4-dimensional, but we wish to keep the fields, mass, and coupling in the same dimensions as before, so we introduce a mass term $\mu_{\text{DS}}^{-2\epsilon}$ into the Lagrangian wherever appropriate. The typical one-loop integral, eq. (6.1), is updated to

$$I_{i_1 \dots i_k}^d [N^{\mu_1 \dots \mu_n}] \equiv \mu_{\text{DS}}^{-2\epsilon} \int \frac{d^d l_{[d]}}{(2\pi)^d} \frac{N^{\mu_1 \dots \mu_n}}{D_{i_1} \dots D_{i_k}}, \quad (6.10)$$

where the integration limits are implicit. The new mass μ_{DS} will eventually appear in a logarithm of the form $\ln(\mu_{\text{DS}}/m)$ for some physical scale m , and physical observables will be independent of the choice of μ_{DS}^2 , at least up to the next order of the perturbative expansion.²⁸ We are free to choose which objects are d -dimensional, and which stay 4-dimensional, with the conventional choice being to make all objects which can lead to singularities like loop particles d -dimensional, keeping external, non-singular objects in 4 dimensions.

The nicest features of dimensional regularisation are that they keep Lorentz symmetry intact, and that the divergences are given by poles in the extra-dimensional parameter ϵ . Taking the 4d limit means taking $\epsilon \rightarrow 0$, and the poles can easily be removed by adding an equal and opposite pole in ϵ into the counterterms of the theory.

However, one major point of difficulty for dimensional regularisation is chirality and γ^5 . In $d = 4 - 2\epsilon$ dimensions, we no longer have the nice separation of spacetime into a **left**- and a **right**-chiral part (cf. section 2.1), and γ^5 is ill-defined.²⁹ Additionally, there is no 4d representation of the Dirac or Lorentz algebras, which are upgraded to formal algebras with relations such as

$$\left\{ \gamma_{[d]}^\mu, \gamma_{[d]}^\nu \right\} = 2g_{[d]}^{\mu\nu}, \quad g_{[d]\mu}^\mu = d = 4 - 2\epsilon. \quad (6.11)$$

Therefore, we are unable to use many of the nice tricks from 4 dimensions such as chirality flow to simplify the spin algebra,³⁰ and calculations instead become more cumbersome.

²⁸This leads to a large amount of physical consequences which are outside the scope of this thesis. If interested please see e.g. [10].

²⁹It should be stressed that this is not actually a problem per se, and that most loop calculations are successfully completed using dimensional regularisation.

³⁰We are hopeful of being able to update the chirality-flow formalism to d -dimensions in future.

6.3 The FDF Formalism

One way around these difficulties is to modify dimensional regularisation by adding a new subspace $QS_{[n_\epsilon]}$ on top of the d -dimensional one, to obtain

$$QS_{[d_s]} \equiv QS_{[d]} \oplus QS_{[n_\epsilon]} = S_{[4]} \oplus QS_{[-2\epsilon]} \oplus QS_{[n_\epsilon]} \equiv S_{[4]} \oplus QS_{[n_\epsilon - 2\epsilon]}, \quad (6.12)$$

where we defined two new spaces, $QS_{[d_s]}$ and $QS_{[n_\epsilon - 2\epsilon]}$. If we take $d_s \rightarrow 4$ then $QS_{[d_s]}$ is an infinite-dimensional space with total size four. It is fundamentally different to Minkowski space, exemplified by the fact that its indices can have non-integer values. Doing this, we have the vector space

$$QS_{[d_s]} = S_{[4]} \oplus QS_{[n_\epsilon - 2\epsilon]}, \quad (6.13)$$

of the FDF formalism [80] which is used in paper IV to calculate one-loop diagrams with chirality flow.

In the FDF formalism, all objects (except for loop momenta and integrals) are four dimensional, with some multiplied by an additional algebra called the -2ϵ -selection rules (-2ϵ -SRs). The -2ϵ -SRs are described in paper IV, can be precalculated in any Feynman diagram, and contribute an overall factor of 0 or ± 1 to the amplitude. After doing the -2ϵ -SRs algebra, the spin-structure of a Feynman diagram only contains four-dimensional quantities and an extra mass³¹ $\mu^2 = -l_{[-2\epsilon]}^2$. This implies that chirality and γ^5 are both well defined, and we can separate spacetime into **left**- and **right**-chiral pieces, making the FDF formalism a good basis to develop chirality flow at one-loop order, as is done in paper IV.

Despite all of the previous discussion of four dimensions, the loop integrals and loop momenta in FDF are actually d -dimensional. Therefore, after simplifying the Lorentz structure we will obtain integrals of the form of eq. (6.10), which obey useful properties like shift symmetries and Lorentz symmetry, and which have well-known solutions. If the integral contains the extra mass μ^2 , we use

$$I_{i_1 \dots i_k}^d [(\mu^2)^r] = (2\pi)^r I_{i_1 \dots i_k}^{d+2r} [1] \prod_{j=0}^{r-1} (d - 4 - 2j), \quad (6.14)$$

to remove the extra-dimensional mass and replace it with a higher-dimensional integral.³²

Finally, we comment that to date the FDF formalism has only been consistently developed for one-loop diagrams. Therefore, unless this is resolved, we will have to adopt a different

³¹Note that the extra dimensions are spacelike, so $l_{[-2\epsilon]}^2$ is a negative number.

³²It is well known how to reduce this back into an integral with $4 - 2\epsilon$ dimensions and no μ^2 dependence [81].

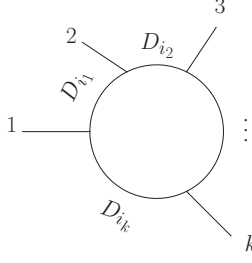


Figure 11: A generic one-loop scalar Feynman diagram.

regularisation scheme to develop chirality flow beyond a single loop. Further, using the FDF method for loops with multiple fermion lines gives the correct result, but contains spurious extra terms which eventually vanish [80].

6.4 Tensor Reduction and Master Integrals

This section deals with solving the loop integral eq. (6.10). The simplest version of this integral is the scalar integral, defined as

$$I_{i_1 \dots i_k}^d[1] \equiv \mu_{\text{DS}}^{-2\epsilon} \int \frac{d^d l_{[d]}}{(2\pi)^d} \frac{1}{D_{i_1} \dots D_{i_k}}, \quad (6.15)$$

which comes from a Feynman diagram with k legs and a single loop (see figure 11). It is well known that all scalar one-loop integrals can be reduced to a set of four master integrals [76, 82–89], for example to eq. (6.15) with $k = 1, 2, 3$, and 4. The master integrals were solved long ago, are typically functions of logarithms, dilogarithms, and the gamma function, and there are many programs which can be used to calculate them (e.g. [89–95]).

If the integral eq. (6.10) has a tensor structure, then its solution will have the same tensor structure, with the tensors being composed of the metric and the momenta in the integral. For example, two tensor integrals present in paper IV are

$$\begin{aligned} \mu_{\text{DS}}^{-2\epsilon} \int \frac{d^d l_{[d]}}{(2\pi)^d} \frac{l_{[d]}^\mu}{(l+1)_{[d]}^2 (l-2)_{[d]}^2} &= C_1 1^\mu + C_2 2^\mu, \\ \mu_{\text{DS}}^{-2\epsilon} \int \frac{d^d l_{[d]}}{(2\pi)^d} \frac{l_{[d]}^\mu l_{[d]}^\nu}{l_{[d]}^2 (l+1)_{[d]}^2 (l-2)_{[d]}^2} &= C_{00} g^{\mu\nu} + C_{11} 1^\mu 1^\nu + C_{22} 2^\mu 2^\nu \\ &\quad + C_{12} (1^\mu 2^\nu + 1^\nu 2^\mu), \end{aligned} \quad (6.16)$$

where we use the shorthand $1^\mu \equiv p_1^\mu$ and $2^\mu \equiv p_2^\mu$, and we leave the dimension of the external momenta 1 and 2 undetermined for flexibility. Note that the second integral has

to be symmetric in μ and ν . The coefficients C_i, C_{ij} are functions of ϵ and the invariants in the process, for example 1^2 or $(1 \cdot 2)$.

To calculate the scalar coefficients of eq. (6.16), we can use e.g. the approaches of Passarino-Veltman [96] or Davydychev [81]. For example, the coefficients of the first integral can be calculated by contracting the equation with 1_μ and 2_μ to obtain an easily solvable set of linear equations,

$$\begin{aligned} C_1 1^2 + C_2 (1 \cdot 2) &= \mu_{\text{DS}}^{-2\epsilon} \int \frac{d^d l_{[d]}}{(2\pi)^d} \frac{l_{[d]} \cdot 1}{(l+1)_{[d]}^2 (l-2)_{[d]}^2} , \\ C_1 (1 \cdot 2) + C_2 2^2 &= \mu_{\text{DS}}^{-2\epsilon} \int \frac{d^d l_{[d]}}{(2\pi)^d} \frac{l_{[d]} \cdot 2}{(l+1)_{[d]}^2 (l-2)_{[d]}^2} . \end{aligned} \quad (6.17)$$

Using that e.g.

$$1 \cdot l_{[d]} = \frac{1}{2} \left[(l+1)_{[d]}^2 - l_{[d]}^2 - 1^2 \right] , \quad (6.18)$$

we can obtain known scalar master integrals on the right-hand-sides of eq. (6.17), thus solving the tensor loop integral.

7 Conclusions and Outlook

In this thesis, I, along with my collaborators, explore ways to optimise scattering amplitude calculations. The main way in which we do this is by introducing and developing the chirality-flow formalism at both tree-level and one-loop-level, while a further paper looks at ways to optimise QCD calculations in MadGraph5_aMC@NLO. It is our hope that chirality flow can become both a widely used and loved analytical tool, and a useful way to optimise current event generators. (We must optimise our event generators to fit into the proposed computer budget of CERN and its experiments [53, 54].)

Through this introduction, I have given a rough overview of both particle physics in general, and the physics involved in each publication. I will now summarise each paper and look ahead to what else can be done following each paper.

Paper I introduced the chirality-flow formalism and showed how to use it to calculate Feynman diagrams in tree-level massless QED and QCD (see sections 2.1.1 and 3.2.1). We showed that chirality flow significantly simplified pen-and-paper calculations of Feynman diagrams. In this paper, we gave a complete and self-consistent set of notation, both in the spinor-helicity method in general, and for chirality flow. This is done so that anyone can use our method without worrying about conflicting conventions. The natural next steps

after this paper were to develop chirality flow for the full Standard Model at tree level and to implement our findings in a computer program, as done in papers II and III respectively. In addition, it would be useful to incorporate Majorana fermions into this formalism; while exploring chirality flow in the context of general amplitude methods, in which Feynman diagrams are skipped, could be interesting.

Paper II developed the chirality-flow formalism for massive particles (see sections 2.1.1 and 3.2.2), thus extending its validity to the full tree-level Standard Model. We showed that while the simplifications of massless theories were nicer, chirality flow still helps significantly simplify Feynman-diagram calculations involving massive particles. At this stage, the obvious next steps were loop diagrams, numerical implementation, higher spins, and Majorana particles. Additionally, it would be interesting to understand chirality flow in the context of the new massive spinor-helicity variables proposed in [43].

Paper III implemented chirality flow for massless QED in MG5aMC (see sections 3.2.1 and 5). We found a very significant improvement in computation speed, up to a factor of 10, compared to the native QED implementation in MG5aMC. Due to the success of this implementation, implementing the rest of the Standard Model in MG5aMC would be very interesting. However, it should be remembered that the main bottleneck in QCD is not the kinematics, but the colour [52]. Nonetheless, making the kinematics faster is still desirable, and pushes the colour bottleneck into an even more prominent position. This extension is ongoing work, involving the authors of paper III and two master students. Also, our program only calculates matrix elements for given phase-space points, and extending it to MadEvent such that it can also calculate cross sections is important for usability. Finally, our implementation is a toy one, and needs significant work to be user friendly and incorporated in the main MG5aMC program.

Paper IV developed chirality flow for general one-loop calculations (see section 6). We built on the four-dimensional formulation [80] of the 4d helicity scheme [97], which allowed all of the useful properties and simplifications of chirality flow from tree-level to be automatically carried over into loop calculations. We found that the Lorentz algebra and the tensor reduction is simplified compared to previous methods. An obvious route forward, is to develop chirality flow for loop calculations using other regularisation schemes such as conventional dimensional regularisation [77–79], which would improve the flexibility of the method, and more easily allow it go to multiple loops.

Finally, paper V explored the benefits of using Berends-Giele recursions to calculate kinematic amplitudes, and of using a colour expansion to approximate matrix elements in MG5aMC (see sections 3.3, 4.1, and 5). We found a speedup of the colour bottleneck of about a factor 2 even at full colour, and that, for most processes, N2LC was both precise and accurate. However, we found that our implementation of Berends-Giele recursions was poor, and can be optimised significantly. Like with chirality flow, there is a large scope

for possible future projects in this direction. Most simply, the new colour implementation can be ported into the standard MG5aMC framework to help alleviate its bottleneck, and the recursion relations can be optimised. Additionally, this paper only calculated matrix elements, and, like in paper III, extending it to MadEvent and cross-section calculations may be useful.

8 Overview of Publications in this Thesis

Here, I briefly summarise each paper in the thesis and specify my individual contributions.

Paper I: The chirality-flow formalism

Andrew Lifson, Christian Reuschle, and Malin Sjödhahl
Eur.Phys.J.C 80 (2020) 1006. E-print: arXiv:2003.05877 [hep-ph]
LU-TP 20-16, MCNET-20-10

This paper was based on Malin Sjödhahl's idea that it should be possible to calculate the kinematic $SL(2, \mathbb{C}) \times SL(2, \mathbb{C})$ part of a scattering amplitude analogously to the colour-flow construction of $SU(3)$. This indeed turned out to be possible, and the new calculation method was dubbed chirality flow.

I did most of the calculations and had key ideas for the implementation and validity of the method, with guiding help from Malin and Christian. Together, we found a way to rewrite the Feynman rules as combinations of dotted and undotted lines, allowing a single-line journey from a Feynman diagram to its spinor inner products. In this paper, we treated massless QED and QCD at tree-level and presented a complete self-consistent set of conventions. I wrote and checked most of the main relations, and was the primary author of sections 4 and 6. We all contributed fairly evenly to the editing and checking procedure.

Paper II: The chirality-flow formalism for the standard model

Joakim Alnefjord, **Andrew Lifson**, Christian Reuschle, and Malin Sjödhahl
Eur.Phys.J.C 81 (2021) 371. E-print: arXiv:2011.10075 [hep-ph]
LU-TP 20-51, MCNET-20-25

This paper was a direct continuation of paper I, extending the scope of the chirality-flow formalism to include massive particles and electroweak interactions, and therefore the full Standard Model at tree-level.

Together with Malin Sjödhahl and Christian Reuschle, I co-supervised Joakim Alnefjord's master thesis, during which he did many of the primary calculations in this paper. I independently checked all of his calculations and did most of the remaining primary work. I investigated the fundamentally different properties of massive and massless particles under the Poincaré group, allowing to understand the four-dimensional spin operator. I also

played a large role in determining the structure of the paper and wrote sections 2.3, 2.4, 3.1, 3.2.1, 3.3.1, and 3.4.1, as well as appendices A.2, B, and C. I also edited much of the paper along with Malin.

Paper III: Automating scattering amplitudes with chirality flow

Andrew Lifson, Christian Reuschle, Malin Sjö Dahl, and Zenny Wettersten
Eur.Phys.J.C 82 (2022) 535. E-print: arXiv:2203.13618 [hep-ph]
LU-TP 22-19, MCNET-22-05

In this paper we implemented the chirality-flow formalism from paper I for QED in MadGraph5_aMC@NLO, finding up to a factor of 10 speed increase in evaluation time.

This paper is the culmination of Zenny Wettersten's master's thesis, which was proposed by me, and was supervised by Malin Sjö Dahl and I. Of the three of us, I was the person with a background in MadGraph5_aMC@NLO, so I was the main lead on the technical side. The primary work was mostly shared by Zenny and I, with me being responsible for changing the diagram generation method to allow fermion propagators to change chirality, updating the model within the HELAS creation stage so that the correct vertices could be used, fixing the loop over all processes and chiralities, writing the external photon wavefunctions, and identifying some bugs in Zenny's code. Due to time pressure and a pre-planned holiday, most of the writing was done by my Malin and Zenny while I was away. Instead, I checked the paper, helped insert references, and wrote some sentences here and there during the editing stage.

Paper IV: One-loop calculations in the chirality-flow formalism

Andrew Lifson, Simon Plätzer, and Malin Sjö Dahl
To be submitted to Eur.Phys.J.C. E-print: arXiv:2303.02125 [hep-ph]
LU-TP 23-01, MCNET-23-03

This paper builds on papers I and II by extending chirality flow to the one-loop level. We did this by using the four-dimensional formulation (FDF) of the four-dimensional helicity scheme as our regularisation method, an idea I had after doing a literature review of one-loop methods.

I did the vast majority of the calculations for the paper with guiding help from Malin and Simon. Together, we showed that it was possible to do one-loop calculations easily and efficiently by using chirality flow in the FDF scheme. This allowed simpler Lorentz

algebra and reduction of tensor integrals. I wrote sections 3 and 4, the abstract, half of the conclusion, and the appendix, which together make up the majority of the paper. I also edited the introduction, conclusion, and section 2.

Paper V: Improving colour computations in MadGraph5_aMC@NLO and exploring a $1/N_c$ expansion

Andrew Lifson and Olivier Mattelaer

Eur.Phys.J.C 82 (2022) 1144. E-print: arXiv:2210.07267 [hep-ph]

CP3-22-42, LU-TP 22-58, MCNET 22-16

This paper was the result of my short-term studentship at Louvain-la-Neuve. We revived an old branch of MG5aMC which calculates the kinematics of tree-level amplitudes using Berends-Giele recursions, and calculates the colour using an expansion in the number of colours. This allowed for a study of the accuracy, speed, and precision of the colour expansion and the new recursions.

I did the majority of the work in this project, which started with Olivier reviving the old branch. After fixing an initial bug, we tested the speed and found that the branch was too slow. Therefore, I proposed and implemented an alternative technical implementation of the code. Once we had passed an optimisation threshold, we explored the physics of the colour expansion. In this stage, I tested the accuracy, precision, and speed of the colour expansion. For the manuscript, I proposed the outline and wrote the initial draft for all parts except for the Conclusions and Appendix C. I also created all of the plots and helped in editing.

9 Overview of Work not in this Thesis

In addition to the five papers included in this thesis, I made additional contributions that are not included in this thesis. I wrote several talks and co-wrote a few conference proceedings (papers VI - VIII); I gave many seminars and conference talks; I taught a MadGraph5_aMC@NLO tutorial at the 2022 MCnet school; I continued my master thesis work and helped edit the resulting paper (paper IX); I proposed a bachelor project on the little group for Samyak Parmar, which I co-supervised; I was on the MCnet student and postdoc committee, during which I helped organise a few conferences, and initiated an online journal club and computer club to help young particle physicists network and learn from each other; and I helped propose and supervise two ongoing master-student projects in which we are extending the chirality-flow implementation in MadGraph5_aMC@NLO in

paper III to include the full Standard Model, officially co-supervising one of them.

In addition to all of this I was active in Lund's doctoral student unions, being the chair and vice chair of NDR (Natural Science Doctoral Student Union), on the election committees of NDR and LDK (Lund's Doctoral Student Union), on the docent committee for NDR, in the general assembly of LDK (its highest decision-making body), and a co-chair of the PhD council at the Department of Astronomy and Theoretical Physics. These were all rewarding roles which gave me invaluable experience.

On the physics side, a summary of the publications not included in this thesis is the following:

Paper VI: A brief look at the chirality-flow formalism for Standard Model amplitudes

Joakim Alnefjord, **Andrew Lifson**, Christian Reuschle, and Malin Sjö Dahl
PoS LHCP2021 (2021) 160. E-print: arXiv:2110.04125 [hep-ph]
LU TP 21-46, MCNET-21-13

This conference proceedings refers to an online talk I gave at LHCP 2020 on the chirality-flow formalism. I wrote the full first draft of the proceedings, which was checked and edited by my collaborators.

Paper VII: Introducing the chirality-flow formalism

Joakim Alnefjord, **Andrew Lifson**, Christian Reuschle, and Malin Sjö Dahl
Acta Phys.Polon.B (2020) 51.

This is the proceedings of a conference talk Malin Sjö Dahl gave at Epiphany 2020. I helped edit the proceedings paper.

Paper VIII: The chirality-flow formalism for Standard Model calculations

Joakim Alnefjord, **Andrew Lifson**, Christian Reuschle, and Malin Sjö Dahl
LT-14 (2022). E-print: arXiv:2204.12324 [hep-ph]

This is the proceedings of a conference talk Malin Sjö Dahl gave at LT-14 in 2021. I helped edit the proceedings paper.

Paper IX: Calculating the primary Lund Plane density

Andrew Lifson, Gavin P. Salam, and Gregory Soyez

JHEP 10 (2020) 170. E-print: [arXiv:2007.06578](https://arxiv.org/abs/2007.06578) [hep-ph]

This paper is the result of my master thesis, which I continued part time in the first year of my PhD. I did a version of most of the calculations in section 3 and helped edit the paper.

References

- [1] S. Weinberg, *The Quantum theory of fields. Vol. 1: Foundations*. Cambridge University Press, 6, 2005.
- [2] M. Maggiore, *A Modern introduction to quantum field theory*. Oxford University Press, September, 2005.
- [3] E. P. Wigner, “On Unitary Representations of the Inhomogeneous Lorentz Group,” *Annals Math.* **40** (1939) 149–204.
- [4] V. Bargmann and E. P. Wigner, “Group Theoretical Discussion of Relativistic Wave Equations,” *Proc. Nat. Acad. Sci.* **34** (1948) 211.
- [5] P. Schuster and N. Toro, “On the Theory of Continuous-Spin Particles: Wavefunctions and Soft-Factor Scattering Amplitudes,” *JHEP* **09** (2013) 104, [arXiv:1302.1198 \[hep-th\]](#).
- [6] P. Schuster and N. Toro, “On the Theory of Continuous-Spin Particles: Helicity Correspondence in Radiation and Forces,” *JHEP* **09** (2013) 105, [arXiv:1302.1577 \[hep-th\]](#).
- [7] P. Schuster and N. Toro, “A Gauge Field Theory of Continuous-Spin Particles,” *JHEP* **10** (2013) 061, [arXiv:1302.3225 \[hep-th\]](#).
- [8] P. Schuster and N. Toro, “Continuous-spin particle field theory with helicity correspondence,” *Phys. Rev. D* **91** (2015) 025023, [arXiv:1404.0675 \[hep-th\]](#).
- [9] R. K. Ellis, W. J. Stirling, and B. Webber, “QCD and collider physics,” *Camb. Monogr. Part. Phys. Nucl. Phys. Cosmol.* **8** (1996) 1–435.
- [10] M. E. Peskin and D. V. Schroeder, *An Introduction to quantum field theory*. Addison-Wesley, Reading, USA, 1995.
<http://www.slac.stanford.edu/~mpeskin/QFT.html>.
- [11] L. J. Dixon, “Calculating scattering amplitudes efficiently.” Arxiv:hep-ph/9601359v2, 1996.
- [12] H. Elvang and Y.-t. Huang, “Scattering Amplitudes,” [arXiv:1308.1697 \[hep-th\]](#).
- [13] C.-N. Yang and R. L. Mills, “Conservation of Isotopic Spin and Isotopic Gauge Invariance,” *Phys. Rev.* **96** (1954) 191–195.
- [14] L. D. Faddeev and V. N. Popov, “Feynman Diagrams for the Yang-Mills Field,” *Phys. Lett. B* **25** (1967) 29–30.

- [15] A. Buckley *et al.*, “General-purpose event generators for LHC physics,” *Phys. Rept.* **504** (2011) 145–233, [arXiv:1101.2599 \[hep-ph\]](#).
- [16] P. Skands, “Introduction to QCD,” in *Theoretical Advanced Study Institute in Elementary Particle Physics: Searching for New Physics at Small and Large Scales*, pp. 341–420. 2013. [arXiv:1207.2389 \[hep-ph\]](#).
- [17] **Particle Data Group** Collaboration, R. L. Workman *et al.*, “Review of Particle Physics,” *PTEP* **2022** (2022) 083C01.
- [18] C. Møller, “General Properties of the Characteristic Matrix in the Theory of Elementary Particles I,” *D. Kgl Danske Vidensk. Selk. Mat.-Fys. Medd.* **23** no. 1, (1945) 48.
- [19] M. Cannoni, “Lorentz invariant relative velocity and relativistic binary collisions,” *Int. J. Mod. Phys. A* **32** no. 02n03, (2017) 1730002, [arXiv:1605.00569 \[hep-ph\]](#).
- [20] F. A. Berends and W. Giele, “The Six Gluon Process as an Example of Weyl-Van Der Waerden Spinor Calculus,” *Nucl. Phys.* **B294** (1987) 700–732.
- [21] M. Dinsdale, M. Ternick, and S. Weinzierl, “A Comparison of efficient methods for the computation of Born gluon amplitudes,” *JHEP* **03** (2006) 056, [arXiv:hep-ph/0602204](#).
- [22] T. Gleisberg, S. Hoeche, F. Krauss, and R. Matyszkiewicz, “How to calculate colourful cross sections efficiently,” [arXiv:0808.3672 \[hep-ph\]](#).
- [23] S. Badger, B. Biedermann, L. Hackl, J. Plefka, T. Schuster, and P. Uwer, “Comparing efficient computation methods for massless QCD tree amplitudes: Closed analytic formulas versus Berends-Giele recursion,” *Phys. Rev. D* **87** no. 3, (2013) 034011, [arXiv:1206.2381 \[hep-ph\]](#).
- [24] P. De Causmaecker, R. Gastmans, W. Troost, and T. T. Wu, “Multiple Bremsstrahlung in Gauge Theories at High-Energies. 1. General Formalism for Quantum Electrodynamics,” *Nucl. Phys. B* **206** (1982) 53–60.
- [25] F. A. Berends, R. Kleiss, P. De Causmaecker, R. Gastmans, and T. T. Wu, “Single Bremsstrahlung Processes in Gauge Theories,” *Phys. Lett. B* **103** (1981) 124–128.
- [26] F. A. Berends, R. Kleiss, P. De Causmaecker, R. Gastmans, W. Troost, and T. T. Wu, “Multiple Bremsstrahlung in Gauge Theories at High-Energies. 2. Single Bremsstrahlung,” *Nucl. Phys. B* **206** (1982) 61–89.
- [27] P. De Causmaecker, R. Gastmans, W. Troost, and T. T. Wu, “Helicity Amplitudes for Massless QED,” *Phys. Lett. B* **105** (1981) 215.

- [28] CALKUL Collaboration, F. A. Berends, R. Kleiss, P. de Causmaecker, R. Gastmans, W. Troost, and T. T. Wu, “Multiple Bremsstrahlung in Gauge Theories at High-energies. 3. Finite Mass Effects in Collinear Photon Bremsstrahlung,” *Nucl. Phys. B* **239** (1984) 382–394.
- [29] G. R. Farrar and F. Neri, “How to Calculate 35640 $O(\alpha^5)$ Feynman Diagrams in Less Than an Hour,” *Phys. Lett. B* **130** (1983) 109–114. [Addendum: *Phys.Lett.B* **152**, 445–445 (1985)].
- [30] R. Kleiss, “The Cross-section for $e^+e^- \rightarrow e^+e^-e^+e^-$,” *Nucl. Phys. B* **241** (1984) 61.
- [31] F. A. Berends, P. H. Daverveldt, and R. Kleiss, “Complete Lowest Order Calculations for Four Lepton Final States in electron-Positron Collisions,” *Nucl. Phys. B* **253** (1985) 441–463.
- [32] J. F. Gunion and Z. Kunszt, “FOUR JET PROCESSES: GLUON-GLUON SCATTERING TO NONIDENTICAL QUARK - ANTI-QUARK PAIRS,” *Phys. Lett. B* **159** (1985) 167.
- [33] J. F. Gunion and Z. Kunszt, “Improved Analytic Techniques for Tree Graph Calculations and the $G g q$ anti- q Lepton anti-Lepton Subprocess,” *Phys. Lett. B* **161** (1985) 333.
- [34] R. Kleiss and W. J. Stirling, “Spinor Techniques for Calculating p anti- $p \rightarrow W^{+-} / Z^0 + \text{Jets}$,” *Nucl. Phys. B* **262** (1985) 235–262.
- [35] K. Hagiwara and D. Zeppenfeld, “Helicity Amplitudes for Heavy Lepton Production in e^+e^- Annihilation,” *Nucl. Phys. B* **274** (1986) 1–32.
- [36] R. Kleiss, “Hard Bremsstrahlung Amplitudes for e^+e^- Collisions With Polarized Beams at LEP / SLC Energies,” *Z. Phys. C* **33** (1987) 433.
- [37] R. Kleiss and W. J. Stirling, “Cross-sections for the Production of an Arbitrary Number of Photons in Electron - Positron Annihilation,” *Phys. Lett. B* **179** (1986) 159–163.
- [38] Z. Xu, D.-H. Zhang, and L. Chang, “Helicity Amplitudes for Multiple Bremsstrahlung in Massless Nonabelian Gauge Theories,” *Nucl. Phys. B* **291** (1987) 392–428.
- [39] S. Dittmaier, “Weyl-van der Waerden formalism for helicity amplitudes of massive particles,” *Phys. Rev. D* **59** (1998) 016007, [arXiv:hep-ph/9805445](#).
- [40] C. Schwinn and S. Weinzierl, “Scalar diagrammatic rules for Born amplitudes in QCD,” *JHEP* **05** (2005) 006, [arXiv:hep-th/0503015](#) [[hep-th](#)].

- [41] S. J. Parke and T. R. Taylor, “An Amplitude for n Gluon Scattering,” *Phys. Rev. Lett.* **56** (1986) 2459.
- [42] M. L. Mangano and S. J. Parke, “Multiparton amplitudes in gauge theories,” *Phys. Rept.* **200** (1991) 301–367, [arXiv:hep-th/0509223 \[hep-th\]](#).
- [43] N. Arkani-Hamed, T.-C. Huang, and Y.-t. Huang, “Scattering amplitudes for all masses and spins,” *JHEP* **11** (2021) 070, [arXiv:1709.04891 \[hep-th\]](#).
- [44] M. Bohm, A. Denner, T. Sack, W. Beenakker, F. A. Berends, and H. Kuijf, “Electroweak Radiative Corrections to $e^+e^- \rightarrow W^+W^-$,” *Nucl. Phys. B* **304** (1988) 463–499.
- [45] S. Weinzierl, “Automated computation of spin- and colour-correlated Born matrix elements,” *Eur. Phys. J. C* **45** (2006) 745–757, [arXiv:hep-ph/0510157 \[hep-ph\]](#).
- [46] R. Kleiss and H. Kuijf, “Multi - Gluon Cross-sections and Five Jet Production at Hadron Colliders,” *Nucl. Phys. B* **312** (1989) 616–644.
- [47] G. ’t Hooft, “A Planar Diagram Theory for Strong Interactions,” *Nucl. Phys. B* **72** (1974) 461.
- [48] F. Maltoni, K. Paul, T. Stelzer, and S. Willenbrock, “Color Flow Decomposition of QCD Amplitudes,” *Phys. Rev. D* **67** (2003) 014026, [arXiv:hep-ph/0209271](#).
- [49] M. L. Mangano, S. J. Parke, and Z. Xu, “Duality and Multi - Gluon Scattering,” *Nucl. Phys. B* **298** (1988) 653–672.
- [50] V. Del Duca, A. Frizzo, and F. Maltoni, “Factorization of tree QCD amplitudes in the high-energy limit and in the collinear limit,” *Nucl. Phys. B* **568** (2000) 211–262, [arXiv:hep-ph/9909464](#).
- [51] V. Del Duca, L. J. Dixon, and F. Maltoni, “New color decompositions for gauge amplitudes at tree and loop level,” *Nucl. Phys. B* **571** (2000) 51–70, [arXiv:hep-ph/9910563](#).
- [52] O. Mattelaer and K. Ostrolenk, “Speeding up MadGraph5_aMC@NLO,” *Eur. Phys. J. C* **81** no. 5, (2021) 435, [arXiv:2102.00773 \[hep-ph\]](#).
- [53] **HEP Software Foundation** Collaboration, T. Aarrestad *et al.*, “HL-LHC Computing Review: Common Tools and Community Software,” in *2022 Snowmass Summer Study*, P. Canal *et al.*, eds. 8, 2020. [arXiv:2008.13636 \[physics.comp-ph\]](#).
- [54] A. Collaboration, “ATLAS Software and Computing HL-LHC Roadmap,” tech. rep., CERN, Geneva, 2022. <http://cds.cern.ch/record/2802918>.

- [55] S. Keppeler and M. Sjödalh, “Orthogonal multiplet bases in $SU(N_c)$ color space,” [JHEP 09 \(2012\) 124](#), [arXiv:1207.0609 \[hep-ph\]](#).
- [56] M. Sjödalh and J. Thorén, “Decomposing color structure into multiplet bases,” [JHEP 09 \(2015\) 055](#), [arXiv:1507.03814 \[hep-ph\]](#).
- [57] M. Sjödalh and J. Thorén, “QCD multiplet bases with arbitrary parton ordering,” [JHEP 11 \(2018\) 198](#), [arXiv:1809.05002 \[hep-ph\]](#).
- [58] J. Alcock-Zeilinger, S. Keppeler, S. Plätzer, and M. Sjödalh, “Wigner $6j$ symbols for $SU(N)$: Symbols with at least two quark-lines,” [arXiv:2209.15013 \[hep-ph\]](#).
- [59] R. Frederix and T. Vitos, “The colour matrix at next-to-leading-colour accuracy for tree-level multi-parton processes,” [JHEP 12 \(2021\) 157](#), [arXiv:2109.10377 \[hep-ph\]](#).
- [60] P. Cvitanovic, “Group theory for Feynman diagrams in non-Abelian gauge theories,” [Phys. Rev. D 14 \(1976\) 1536–1553](#).
- [61] P. Cvitanovic, P. G. Lauwers, and P. N. Scharbach, “Gauge Invariance Structure of Quantum Chromodynamics,” [Nucl. Phys. B 186 \(1981\) 165–186](#).
- [62] P. Cvitanovic, P. G. Lauwers, and P. N. Scharbach, “The Planar Sector of Field Theories,” [Nucl. Phys. B 203 \(1982\) 385–412](#).
- [63] M. L. Mangano, M. Moretti, F. Piccinini, R. Pittau, and A. D. Polosa, “ALPGEN, a generator for hard multiparton processes in hadronic collisions,” [JHEP 07 \(2003\) 001](#), [arXiv:hep-ph/0206293](#).
- [64] T. Gleisberg and S. Hoeche, “Comix, a new matrix element generator,” [JHEP 12 \(2008\) 039](#), [arXiv:0808.3674 \[hep-ph\]](#).
- [65] A. Cafarella, C. G. Papadopoulos, and M. Worek, “Helac-Phegas: A Generator for all parton level processes,” [Comput. Phys. Commun. 180 \(2009\) 1941–1955](#), [arXiv:0710.2427 \[hep-ph\]](#).
- [66] J. Alwall, R. Frederix, S. Frixione, V. Hirschi, F. Maltoni, O. Mattelaer, H. S. Shao, T. Stelzer, P. Torrielli, and M. Zaro, “The automated computation of tree-level and next-to-leading order differential cross sections, and their matching to parton shower simulations,” [JHEP 07 \(2014\) 079](#), [arXiv:1405.0301 \[hep-ph\]](#).
- [67] M. Moretti, T. Ohl, and J. Reuter, “O’Mega: An Optimizing matrix element generator,” [arXiv:hep-ph/0102195](#).
- [68] W. Kilian, T. Ohl, and J. Reuter, “WHIZARD: Simulating Multi-Particle Processes at LHC and ILC,” [Eur. Phys. J. C 71 \(2011\) 1742](#), [arXiv:0708.4233 \[hep-ph\]](#).

- [69] H. Murayama, I. Watanabe, and K. Hagiwara, “HELAS: HELicity amplitude subroutines for Feynman diagram evaluations,”.
- [70] C. Degrande, C. Duhr, B. Fuks, D. Grellscheid, O. Mattelaer, and T. Reiter, “UFO - The Universal FeynRules Output,” *Comput. Phys. Commun.* **183** (2012) 1201–1214, [arXiv:1108.2040 \[hep-ph\]](#).
- [71] P. de Aquino, W. Link, F. Maltoni, O. Mattelaer, and T. Stelzer, “ALOHA: Automatic Libraries Of Helicity Amplitudes for Feynman Diagram Computations,” *Comput. Phys. Commun.* **183** (2012) 2254–2263, [arXiv:1108.2041 \[hep-ph\]](#).
- [72] N. D. Christensen and C. Duhr, “FeynRules - Feynman rules made easy,” *Comput. Phys. Commun.* **180** (2009) 1614–1641, [arXiv:0806.4194 \[hep-ph\]](#).
- [73] A. Alloul, N. D. Christensen, C. Degrande, C. Duhr, and B. Fuks, “FeynRules 2.0 - A complete toolbox for tree-level phenomenology,” *Comput. Phys. Commun.* **185** (2014) 2250–2300, [arXiv:1310.1921 \[hep-ph\]](#).
- [74] T. Kinoshita, “Mass singularities of Feynman amplitudes,” *J. Math. Phys.* **3** (1962) 650–677.
- [75] T. D. Lee and M. Nauenberg, “Degenerate Systems and Mass Singularities,” *Phys. Rev.* **133** (1964) B1549–B1562.
- [76] G. Heinrich, “Introduction to Loop Calculations,” 2010. <https://www.ippp.dur.ac.uk/~gudrun/teaching/ILC.pdf>.
- [77] C. G. Bollini and J. J. Giambiagi, “Dimensional Renormalization: The Number of Dimensions as a Regularizing Parameter,” *Nuovo Cim. B* **12** (1972) 20–26.
- [78] G. ’t Hooft and M. J. G. Veltman, “Regularization and Renormalization of Gauge Fields,” *Nucl. Phys. B* **44** (1972) 189–213.
- [79] P. Breitenlohner and D. Maison, “Dimensional Renormalization and the Action Principle,” *Commun. Math. Phys.* **52** (1977) 11–38.
- [80] R. A. Fazio, P. Mastrolia, E. Mirabella, and W. J. Torres Bobadilla, “On the Four-Dimensional Formulation of Dimensionally Regulated Amplitudes,” *Eur. Phys. J. C* **74** no. 12, (2014) 3197, [arXiv:1404.4783 \[hep-ph\]](#).
- [81] A. I. Davydychev, “A Simple formula for reducing Feynman diagrams to scalar integrals,” *Phys. Lett. B* **263** (1991) 107–111.
- [82] D. B. Melrose, “Reduction of Feynman diagrams,” *Nuovo Cim.* **40** (1965) 181–213.

- [83] W. L. van Neerven and J. A. M. Vermaseren, “LARGE LOOP INTEGRALS,” *Phys. Lett. B* **137** (1984) 241–244.
- [84] Z. Bern, L. J. Dixon, and D. A. Kosower, “Dimensionally regulated one loop integrals,” *Phys. Lett. B* **302** (1993) 299–308, [arXiv:hep-ph/9212308](#). [Erratum: *Phys.Lett.B* **318**, 649 (1993)].
- [85] Z. Bern, L. J. Dixon, and D. A. Kosower, “Dimensionally regulated pentagon integrals,” *Nucl. Phys. B* **412** (1994) 751–816, [arXiv:hep-ph/9306240](#).
- [86] T. Binoth, J. P. Guillet, and G. Heinrich, “Reduction formalism for dimensionally regulated one loop N point integrals,” *Nucl. Phys. B* **572** (2000) 361–386, [arXiv:hep-ph/9911342](#).
- [87] G. Duplancic and B. Nizic, “Reduction method for dimensionally regulated one loop N point Feynman integrals,” *Eur. Phys. J. C* **35** (2004) 105–118, [arXiv:hep-ph/0303184](#).
- [88] W. T. Giele and E. W. N. Glover, “A Computational formalism for one loop integrals,” *JHEP* **04** (2004) 029, [arXiv:hep-ph/0402152](#).
- [89] R. K. Ellis and G. Zanderighi, “Scalar one-loop integrals for QCD,” *JHEP* **02** (2008) 002, [arXiv:0712.1851 \[hep-ph\]](#).
- [90] R. Mertig, M. Bohm, and A. Denner, “FEYN CALC: Computer algebraic calculation of Feynman amplitudes,” *Comput. Phys. Commun.* **64** (1991) 345–359.
- [91] G. J. van Oldenborgh, “FF: A Package to evaluate one loop Feynman diagrams,” *Comput. Phys. Commun.* **66** (1991) 1–15.
- [92] A. van Hameren, “OneLooP: For the evaluation of one-loop scalar functions,” *Comput. Phys. Commun.* **182** (2011) 2427–2438, [arXiv:1007.4716 \[hep-ph\]](#).
- [93] H. H. Patel, “Package-X: A Mathematica package for the analytic calculation of one-loop integrals,” *Comput. Phys. Commun.* **197** (2015) 276–290, [arXiv:1503.01469 \[hep-ph\]](#).
- [94] H. H. Patel, “Package-X 2.0: A Mathematica package for the analytic calculation of one-loop integrals,” *Comput. Phys. Commun.* **218** (2017) 66–70, [arXiv:1612.00009 \[hep-ph\]](#).
- [95] V. Shtabovenko, “FeynHelpers: Connecting FeynCalc to FIRE and Package-X,” *Comput. Phys. Commun.* **218** (2017) 48–65, [arXiv:1611.06793 \[physics.comp-ph\]](#).

- [96] G. Passarino and M. J. G. Veltman, “One Loop Corrections for $e^+ e^-$ Annihilation Into $\mu^+ \mu^-$ in the Weinberg Model,” *Nucl. Phys. B* **160** (1979) 151–207.
- [97] Z. Bern and A. G. Morgan, “Massive loop amplitudes from unitarity,” *Nucl. Phys. B* **467** (1996) 479–509, [arXiv:hep-ph/9511336](#).

